SUPPORTING INFORMATION

Discovery of Novel Tubulin CBSI (*R*)-9k from Indanone Scaffold for the Treatment of Colorectal Cancer

Zhipeng Huo,[a] Delin Min,[a] Shijie Zhang,[a] Mei-Lin Tang,*[a] and Xun Sun*[ab]

Table of Contents

2.2.10 Molecular Dynamics (MD) Simulation

To better comprehend the activity results and explore related SARs, 300 ns MD simulations were performed for the representative compounds **(*R*)-9k** and **(*S*)-9k**, respectively. In this computational study, we aimed to investigate their binding modes with the colchicine site in tubulin (PDB Code: 1SA0) using Desmond, Schrodinger suites 2022-1 with default settings.[1,2]

2.2.10.1 Ligand Induced Structural Stability

In order to compare the structural effects of both compounds (**(*R*)-9k** and **(*S*)-9k**) when bound at the colchicine binding site, we looked into the structural dynamics of the proteins by estimating the root mean square deviation (RMSD), fluctuation (RMSF) as RMSD and RMSF analysis could reveal the dynamics and motions of constituent atoms and per-residue fluctuation, respectively.

As illustrated in Fig. S1A, **(*R*)-9k** (shown in red) presented a substantially constant RMSD value during simulation, while **(*S*)-9k** (shown in blue) displayed a fluctuating variation between 1.0 and 2.0 Å. Compared with **(*S*)-9k** bound system, the protein was structurally more stable in the presence of **(*R*)-9k** with a relatively steady RMSD value (3.0 Å) (Fig. S1B). In other words, the binding of **(*R*)-9k** in this region could be more settled than that of **(*S*)-9k**. In addition, we further measured relative motions of both compounds at the tubulin dimers over the simulation period. Notably, the motions of specific individual residues in tubulin dimers were higher in the presence of **(*R*)-9k**, likely due to complementary interactions mediated by the compound. However, specific individual residues in the colchicine binding site did not show a significant difference in the presence of **(*R*)-9k** or **(*S*)-9k** (Fig. S1C).

2.2.10.2 Differential Binding Mechanisms Study of (S)-9k and (R)-9k to Tubulin Colchicine Site

While analyzing the dynamics and structural motions of the target protein in the existence of binding agents, we also investigated the molecular mechanics with generalized Born surface area (MM-GBSA) scoring analyses (ΔG, kcal/mol), representing ligand binding affinities to the colchicine binding site. As shown in Table S1, a lower ΔG_{bind} was associated with the binding of **(*R*)-9k** at the colchicine binding site, compared with **(*S*)-9k**, and such a significant energy difference (−7.83 kcal/mol) could be sufficient to support that **(*R*)-9k** bound to colchicine binding site with a higher affinity than **(*S*)-9k**. Regarding the energy contributions from various interactions, coulomb energies changed from −6.72 kcal/mol for **(*S*)-9k** to −10.61 kcal/mol for **(*R*)-**

9k, while both π-π packing and Van der Waals energies varied in the same direction by 0.82 and 3.05 kcal/mol, respectively. These results indicated the high affinity binding of **(*R*)-9k** was mostly influenced by coulomb, vdW and π-π stacking energies relative to **(*S*)-9k**. The calculation of lipophilic energy (ΔG_{lipo}) also supported that the binding of **(*R*)-9k** was more advantageous in the hydrophobic colchicine binding site compared to **(*S*)-9k**.

2.2.10.3 Molecular Docking

The binding mode and key interactions between **(*R*)-9k** and tubulin (PDB code: 1SA0) were investigated by molecular docking. As depicted in Fig. S2A, the hydrogen bond formed between the 9-carbonyl group of cyclo-hepta-trienone in colchicine with Val 181 (shown in yellow dashed line) was replaced by introducing the fluorine atom at the 3-phenyl ring of **(*R*)-9k** (shown in yellow). Meantime, **(*R*)-9k** could form additional hydrogen bonds with water molecules from the methoxy group in A ring and the ethoxy group at the 3-phenyl ring. Further analysis of the docking results (Fig. S2B) showed that the fluorine atom of **(*R*)-9k** fully superimposed with the tropolone of colchicine (shown in red) and the cavity at the binding site of the fluorine atom was too narrow and small to accommodate any larger substituents, which could explain the SARs we observed.

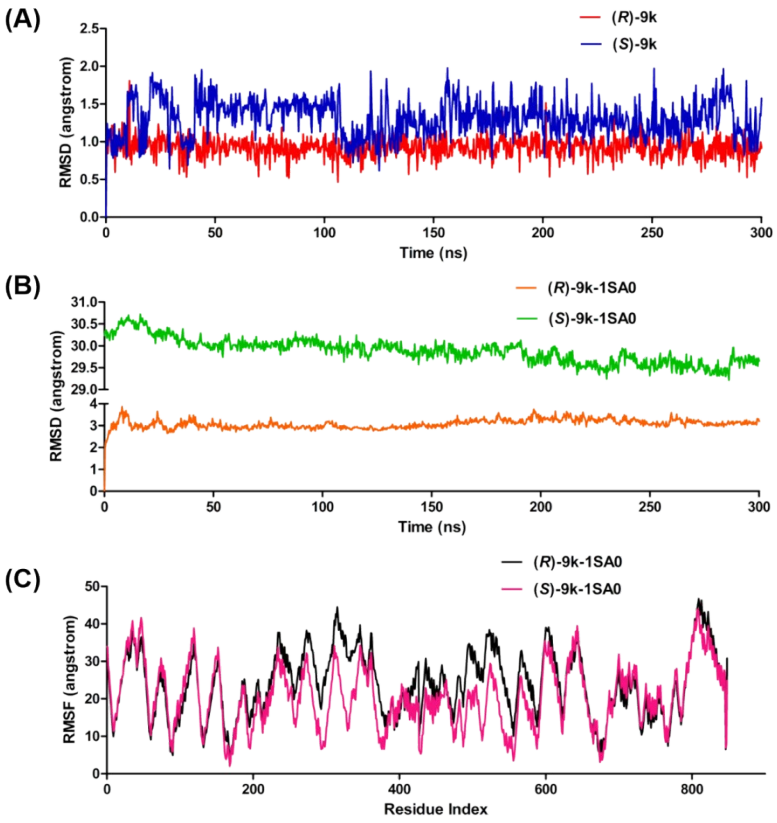

Fig. S1 (A) RMSD graph for the 300 ns simulation trajectory of (*R*)-9k and (*S*)-9k. (B) RMSD graph for the 300 ns simulation trajectory of (*R*)-9k/1SA0 complex and (*S*)-9k/1SA0 complex. (C) RMSF graph for the 300 ns simulation trajectory of (*R*)-9k/1SA0 complex and (*S*)-9k/1SA0 complex.

Table S1 MM/GBSA energy calculations.

Binding energies (kcal/mol)	ΔG_Bind	ΔG_Bind _Coulomb	ΔG_Bind _Covalent	ΔG_Bind _Lipo	ΔG_Bind _Packing	ΔG_Bind _Solv_GB	ΔG_Bind _vdW
(*S*)-9k	-40.05	-6.72	1.97	-13.78	-0.3	17.79	-38.65
(*R*)-9k	-47.88	-10.61	2.69	-15.13	-1.12	18.37	-41.70

ΔG_Bind = total binding free energy; ΔG_Bind_Coulomb = coulomb energy; ΔG_Bind_Covalent = covalent binding energy; ΔG_Bind_Lipo = lipophilic energy; ΔG_Bind_Packing=Pi-pi packing correction; ΔG_Bind_Solv_GB = Generalized Born electrostatic solvation energy; ΔG_Bind_vdW = Van der Waals energy.

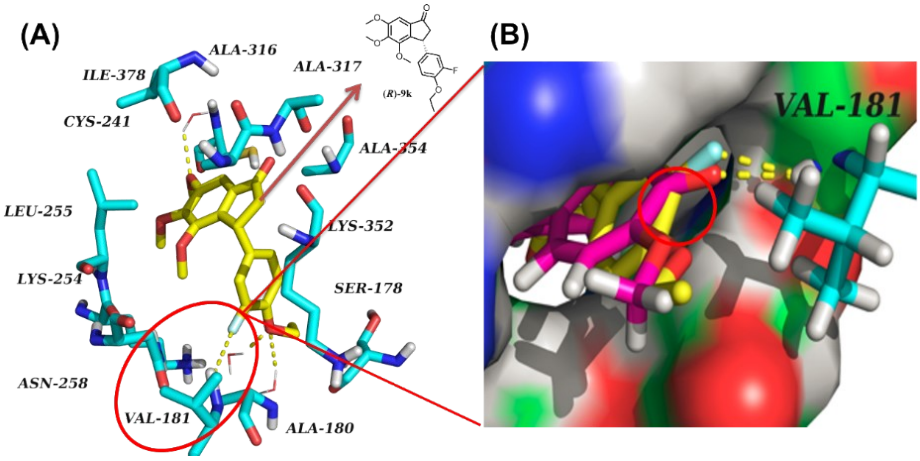

Fig. S2 (A) Proposed binding mode of (*R*)-9k (yellow stick) with tubulin (PDB code: 1SA0). (B) Overlapping between colchicine (red stick) and (*R*)-9k, hydrogen bonds are shown as yellow dashed lines.

References

1 M. Saurov, N. Tufan, B. Kunal et al., *Front Pharmacol.*, 2022, **13**, 805344.

2 J. Li, R. Abel and K. Zhu, et al., *Proteins*, 2011, **79**, 2794-2812.

Compounds **9a-q** were fully characterized by ^{1}H NMR, ^{13}C NMR and HRMS.

4,5,6-Trimethoxy-3-(4-methoxyphenyl)-2,3-dihydro-1H-inden-1-one (**9a**)

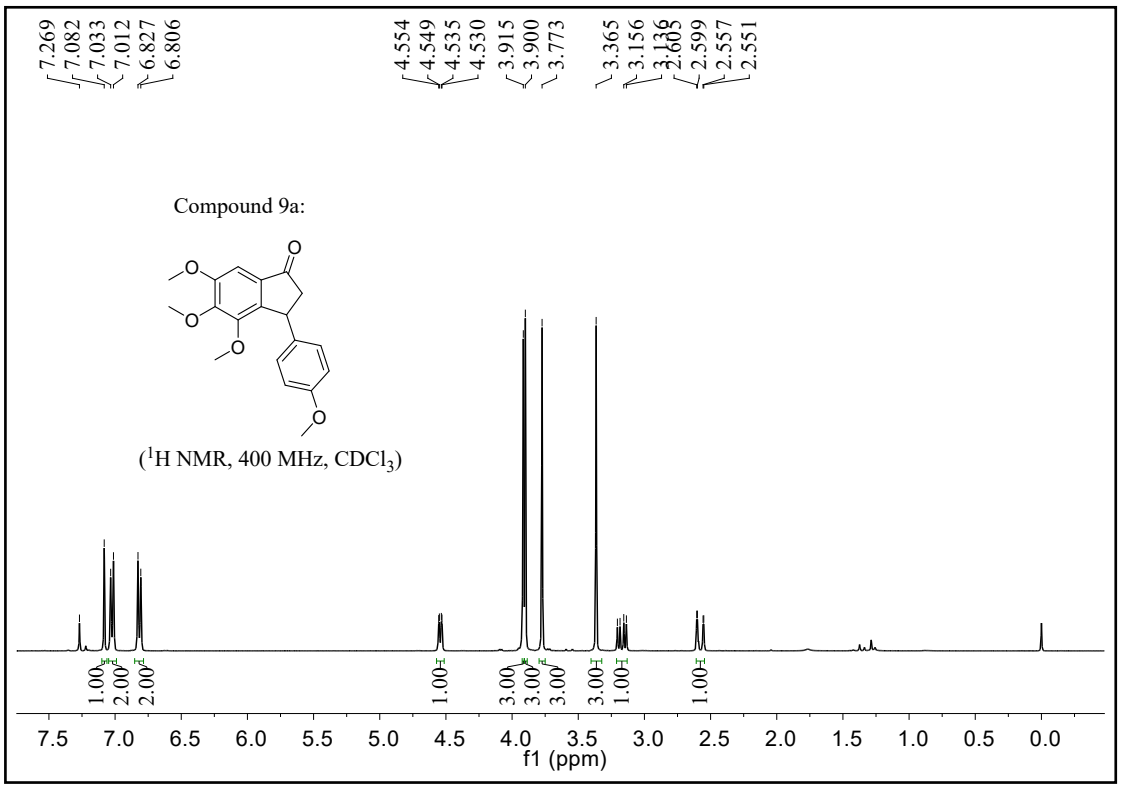

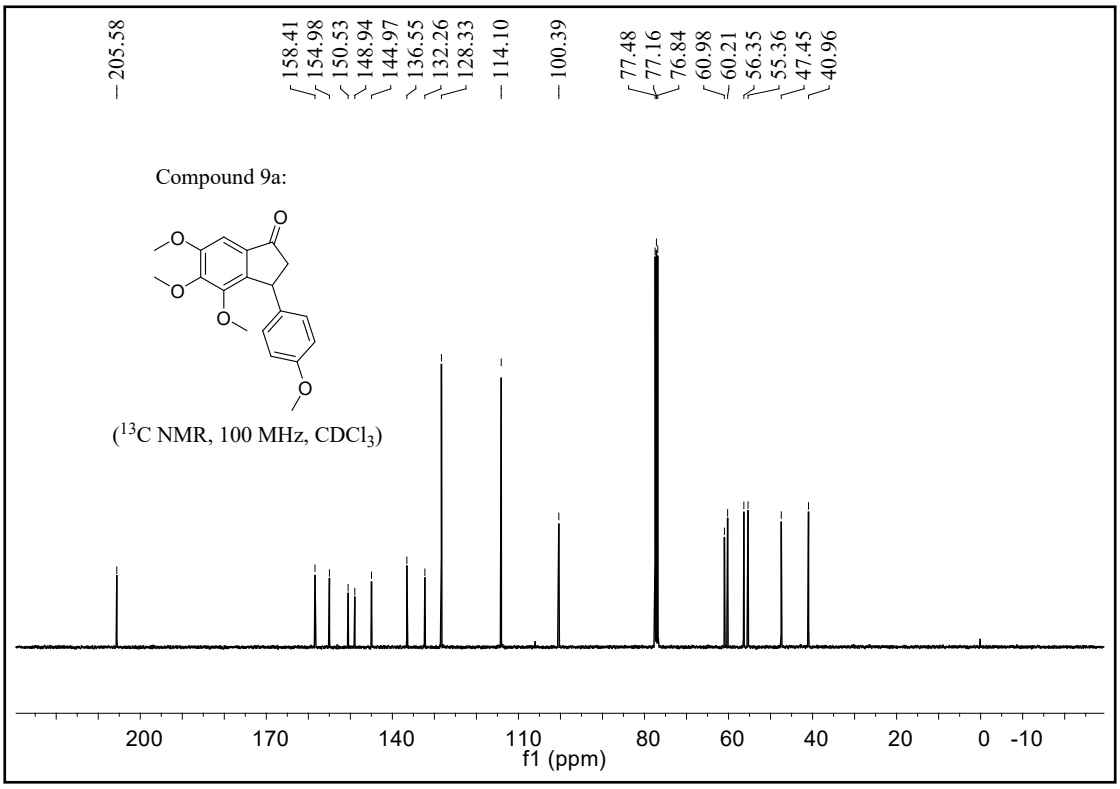

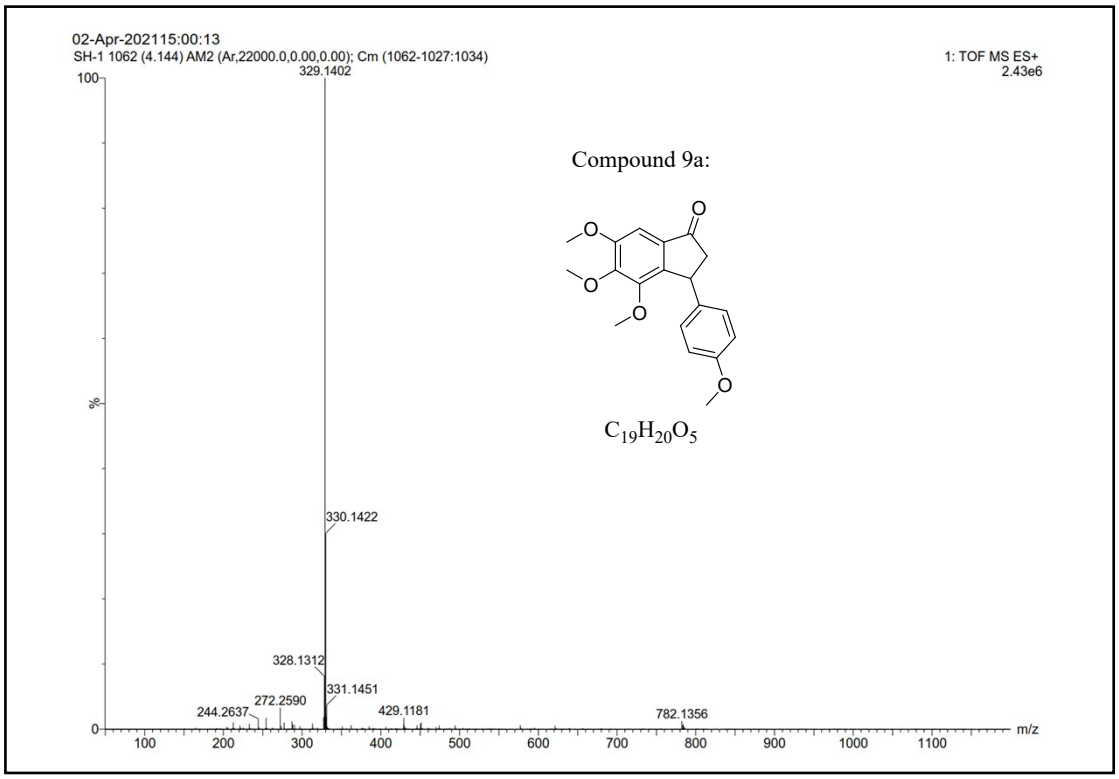

3-(3-Fluoro-4-methoxyphenyl)-4,5,6-trimethoxy-2,3-dihydro-1H-inden-1-one (**9b**)

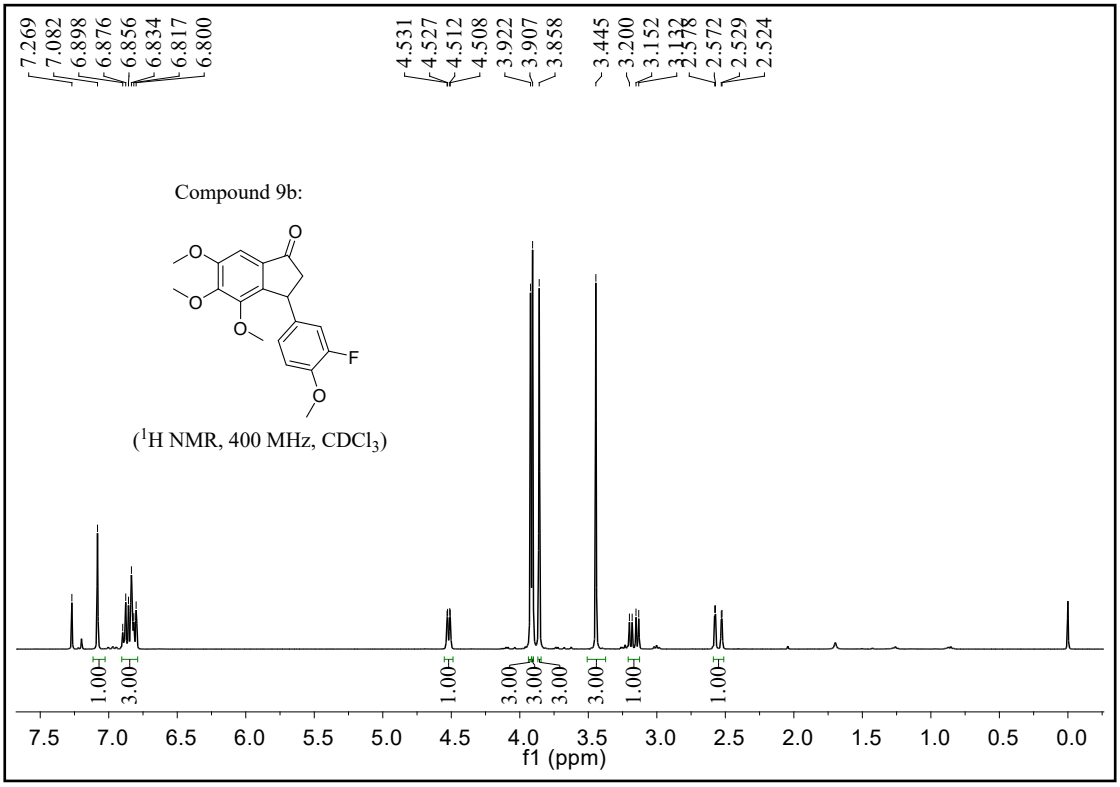

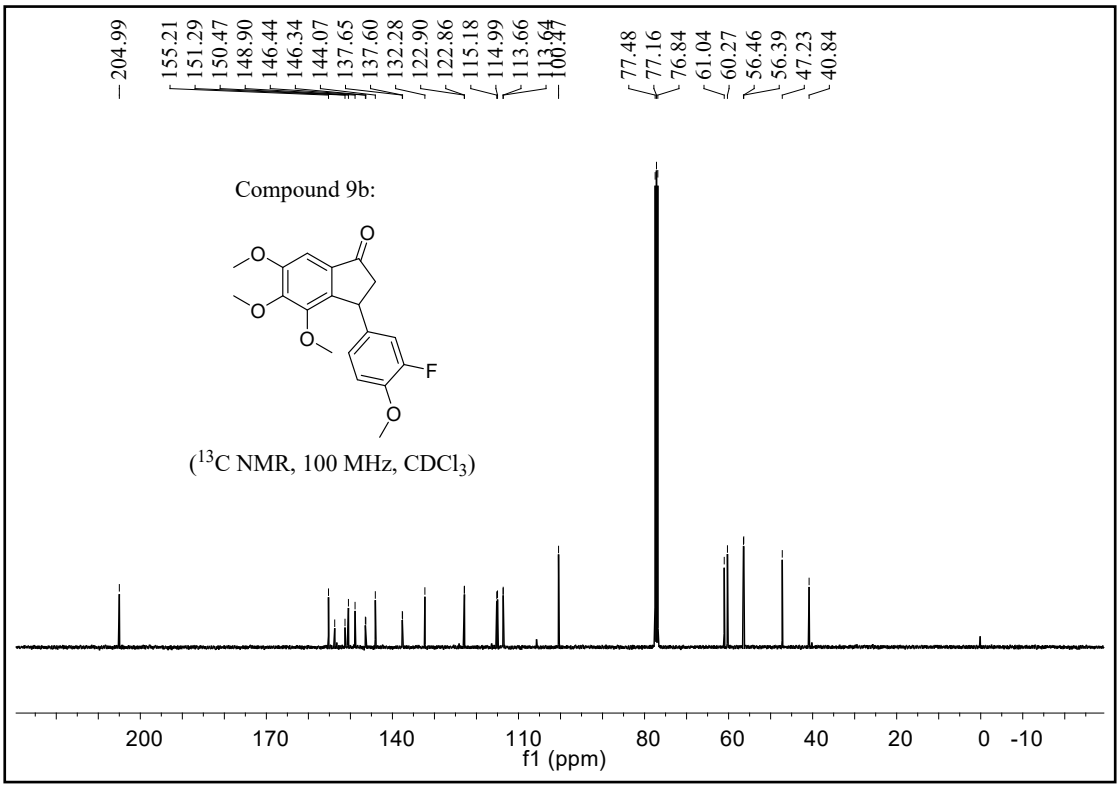
204.99
155.21
151.29
150.47
148.90
146.44
146.34
144.07
137.65
137.60
132.28
122.90
122.86
115.18
114.99
113.66
113.64
100.47
77.48
77.16
76.84
61.04
60.27
56.46
56.39
47.23
40.84
Compound 9b:
O
O
O
O
F
O
(^{13}C NMR, 100 MHz, $CDCl_3$)
200
170
140
110
80
60
40
20
0
-10
f1 (ppm)

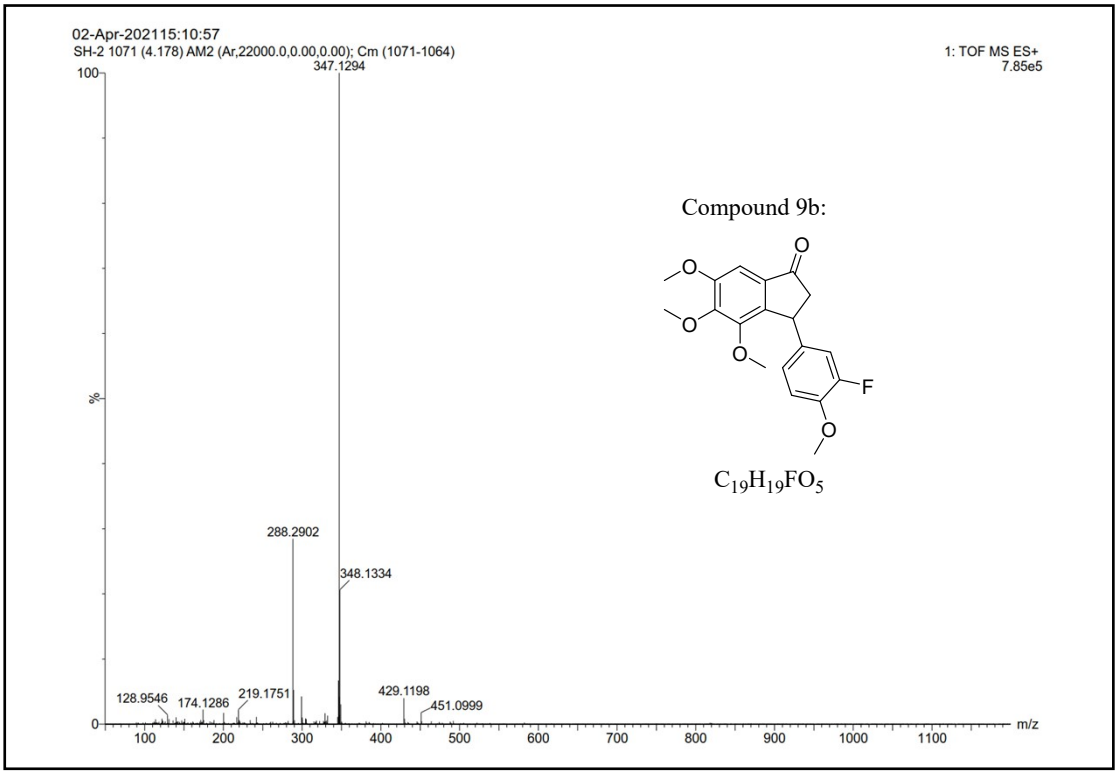
02-Apr-202115:10:57
SH-2 1071 (4.178) AM2 (Ar,22000.0,0.00,0.00); Cm (1071-1064)
1: TOF MS ES+
7.85e5
347.1294
100
%
0
288.2902
348.1334
128.9546
174.1286
219.1751
429.1198
451.0999
100
200
300
400
500
600
700
800
900
1000
1100
m/z
Compound 9b:
O
O
O
O
F
O
$C_{19}H_{19}FO_5$

3-(3-Chloro-4-methoxyphenyl)-4,5,6-trimethoxy-2,3-dihydro-1H-inden-1-one (**9c**)

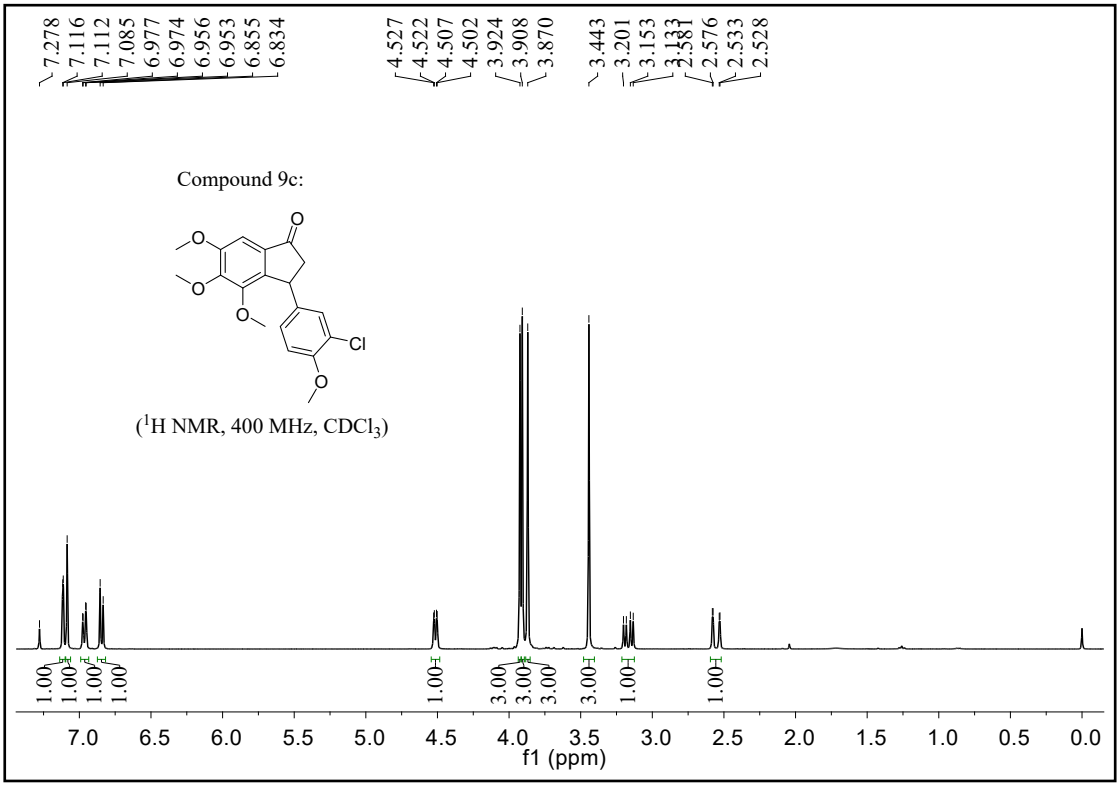

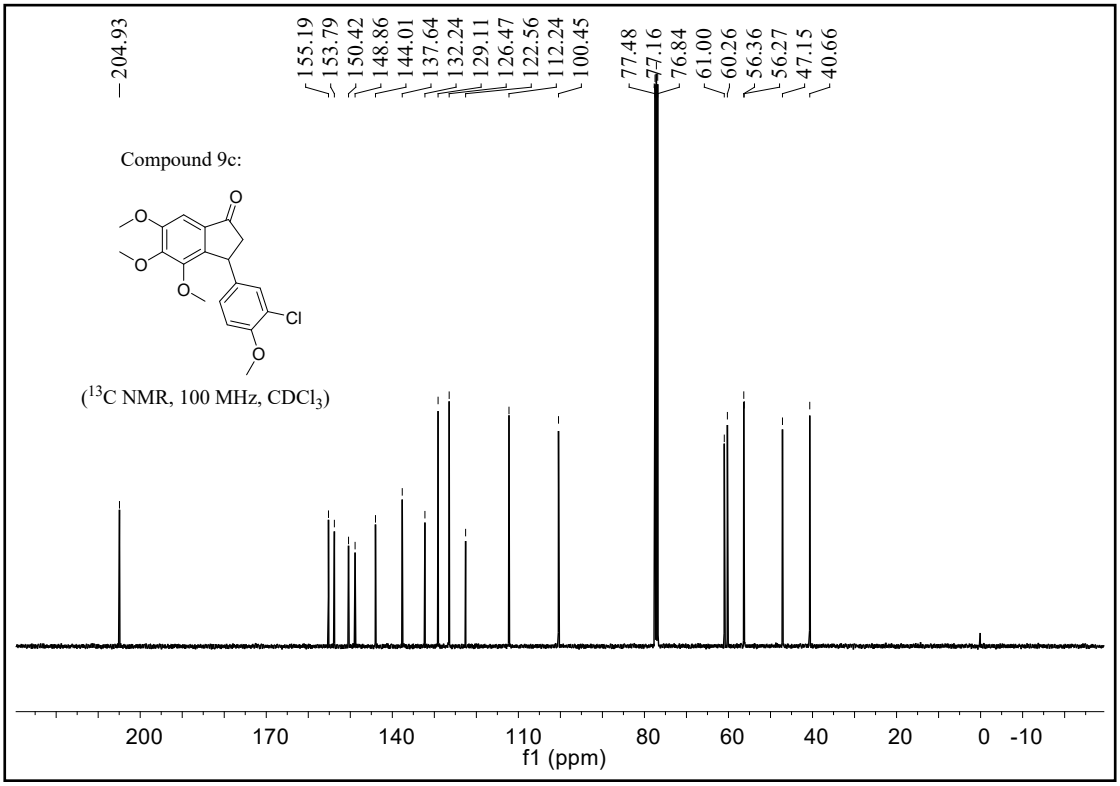

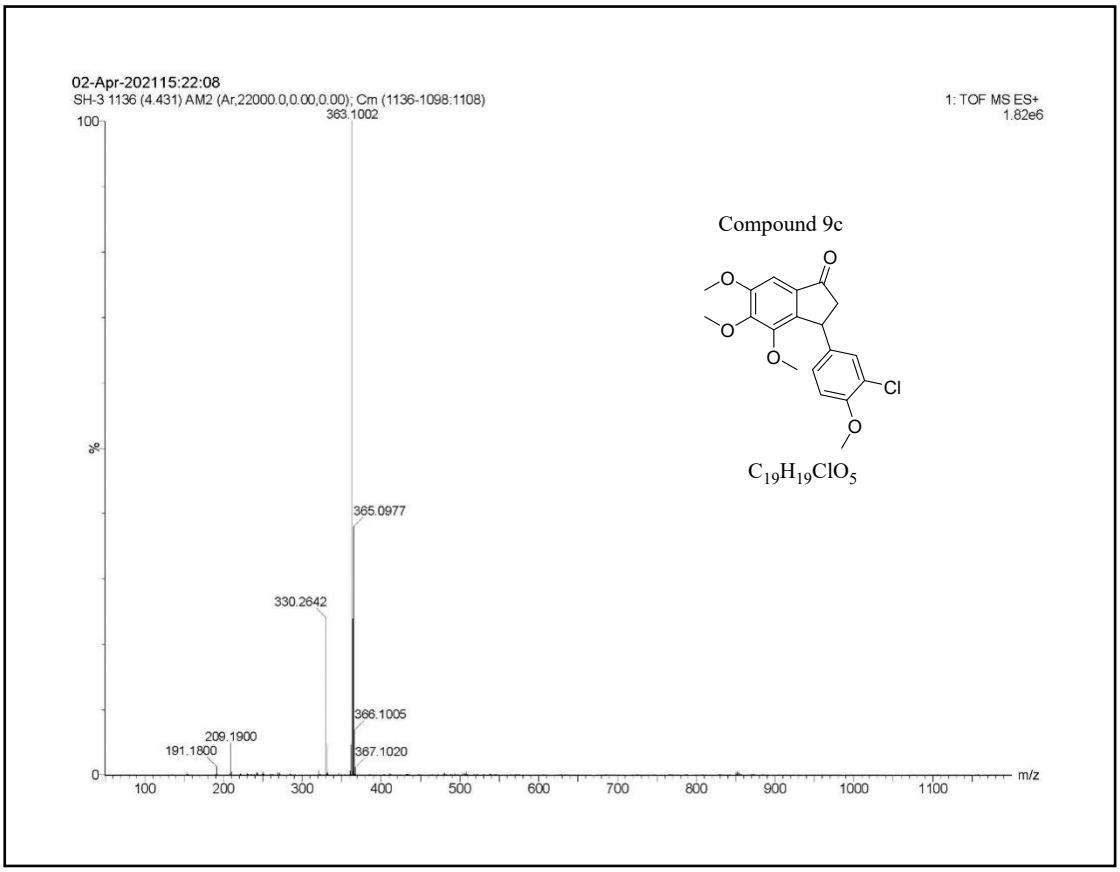

3-(3-Bromo-4-methoxyphenyl)-4,5,6-trimethoxy-2,3-dihydro-1H-inden-1-one (**9d**)

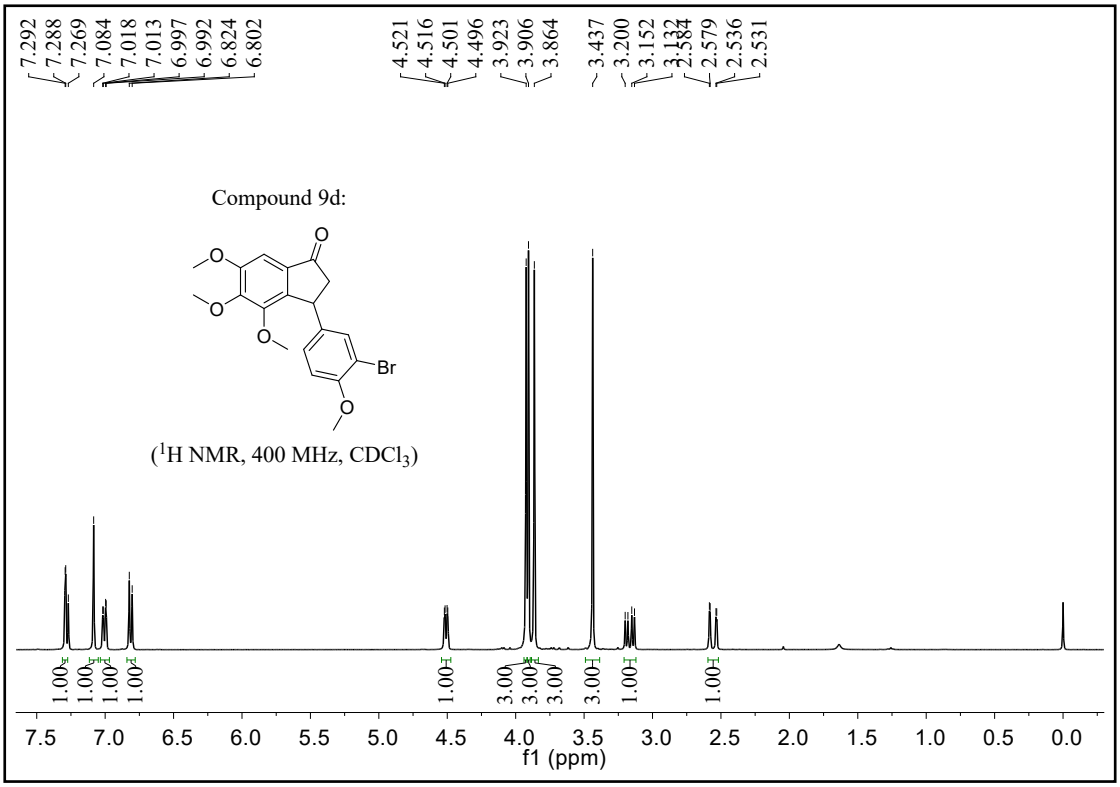

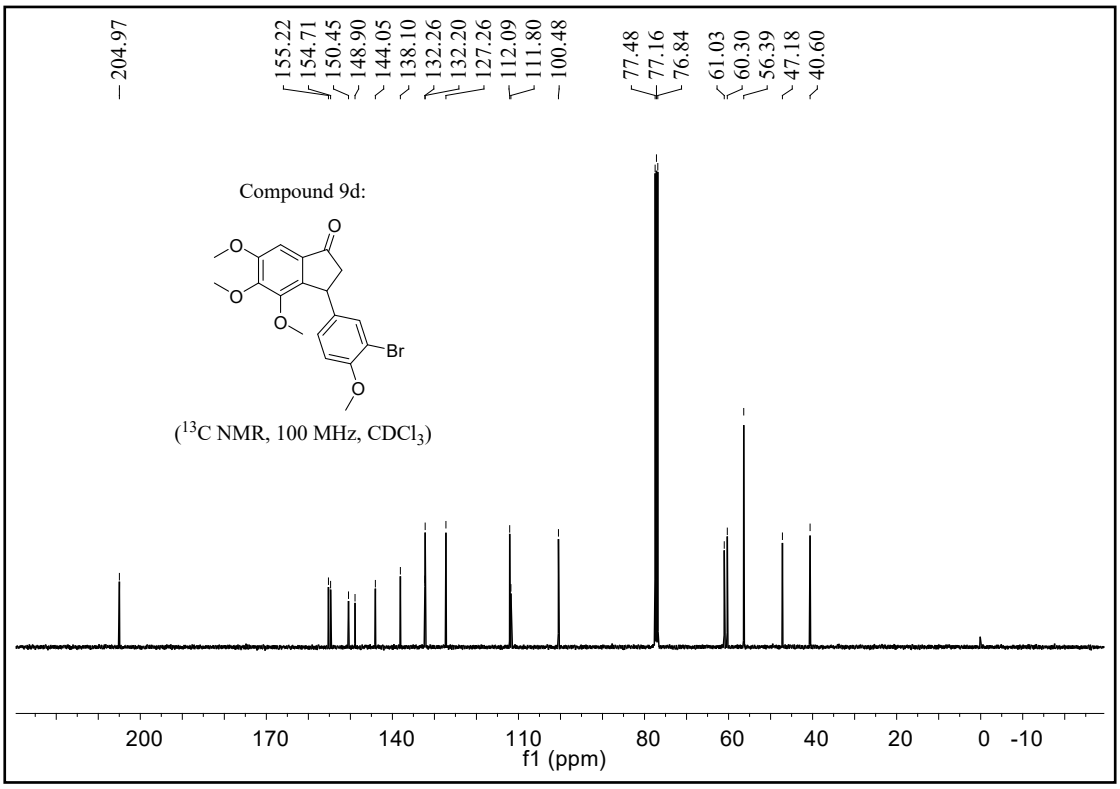
204.97
155.22
154.71
150.45
148.90
144.05
138.10
132.26
132.20
127.26
112.09
111.80
100.48
77.48
77.16
76.84
61.03
60.30
56.39
47.18
40.60
Compound 9d:
O
O
O
O
Br
O
(13C NMR, 100 MHz, CDCl3)
200
170
140
110
80
60
40
20
0
-10
f1 (ppm)

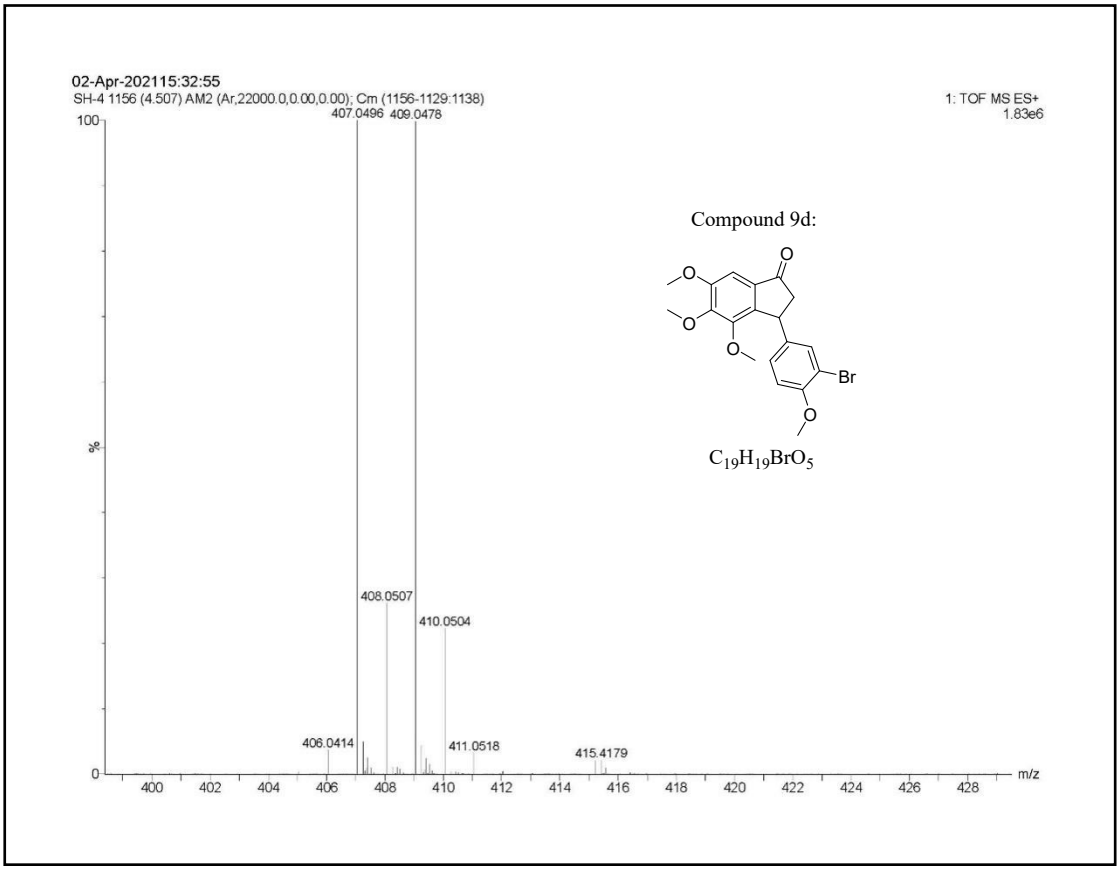
02-Apr-202115:32:55
SH-4 1156 (4.507) AM2 (Ar,22000.0,0.00,0.00); Cm (1156-1129:1138)
1: TOF MS ES+
1.83e6
100
%
0
407.0496
409.0478
408.0507
410.0504
406.0414
411.0518
415.4179
m/z
400
402
404
406
408
410
412
414
416
418
420
422
424
426
428
Compound 9d:
O
O
O
O
Br
O
C19H19BrO5

3-(3-Iodo-4-methoxyphenyl)-4,5,6-trimethoxy-2,3-dihydro-1H-inden-1-one (**9e**)

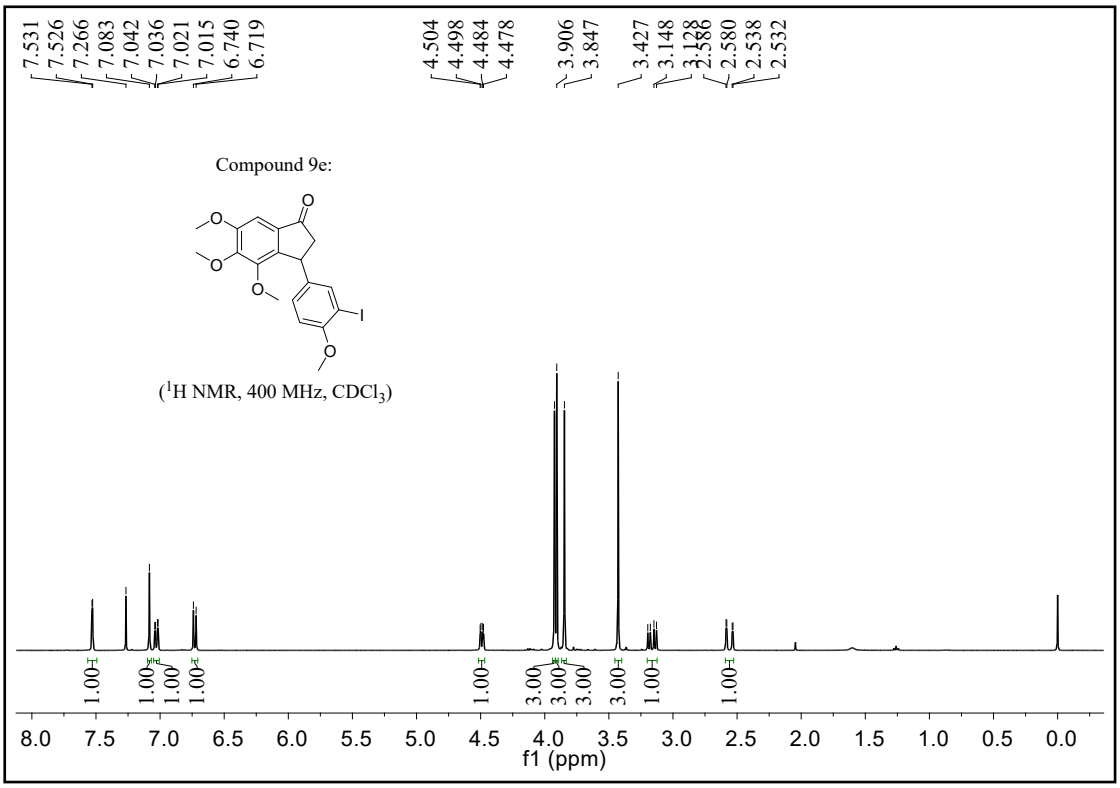

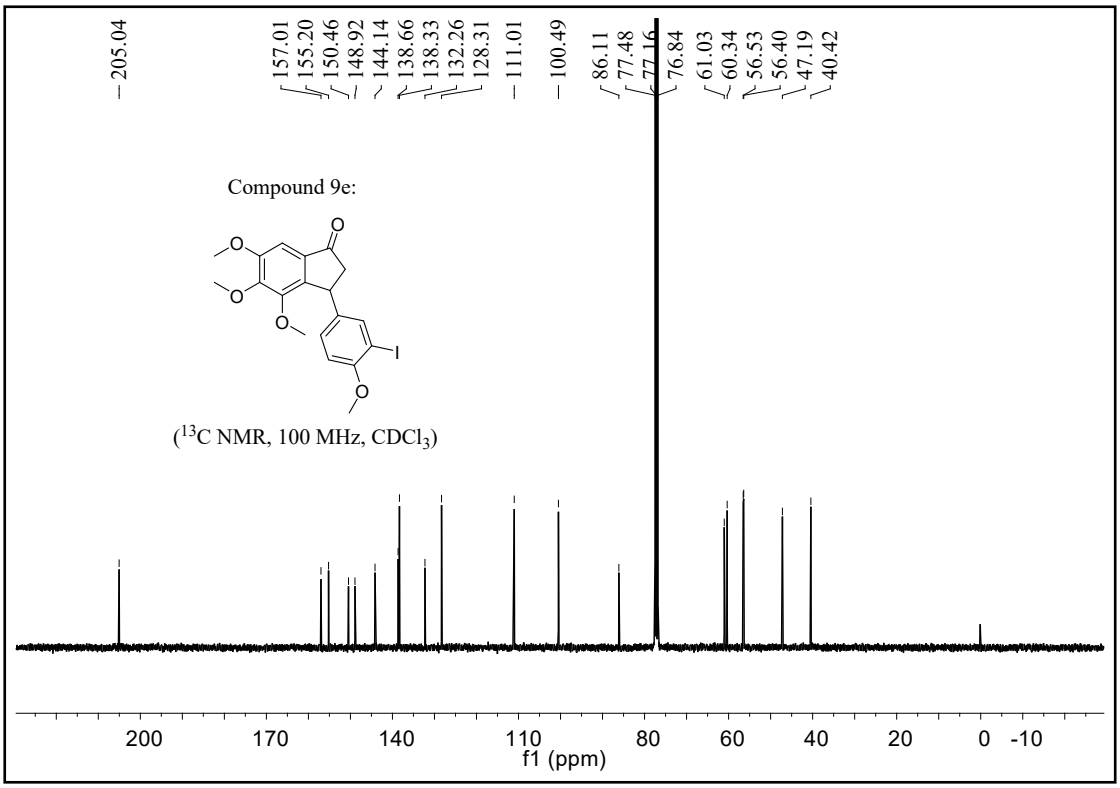

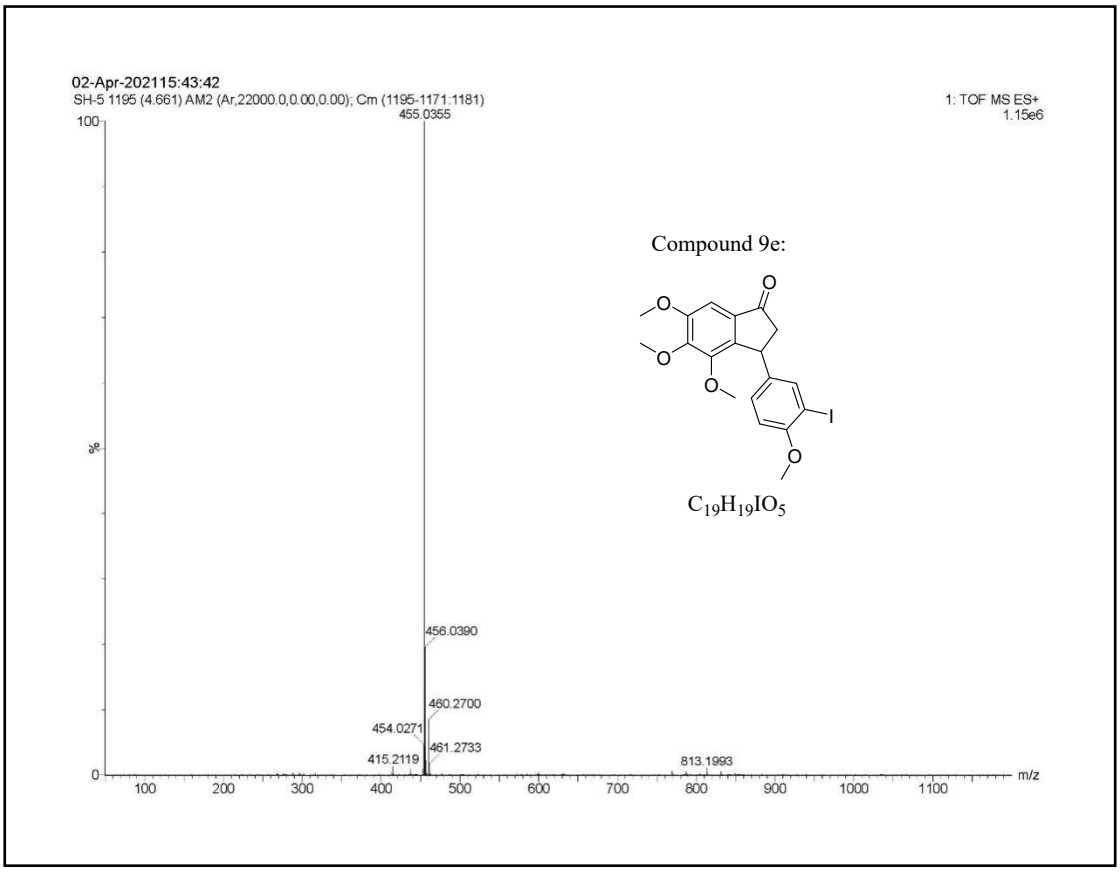

4,5,6-Trimethoxy-3-(4-methoxy-3-nitrophenyl)-2,3-dihydro-1H-inden-1-one (**9f**)

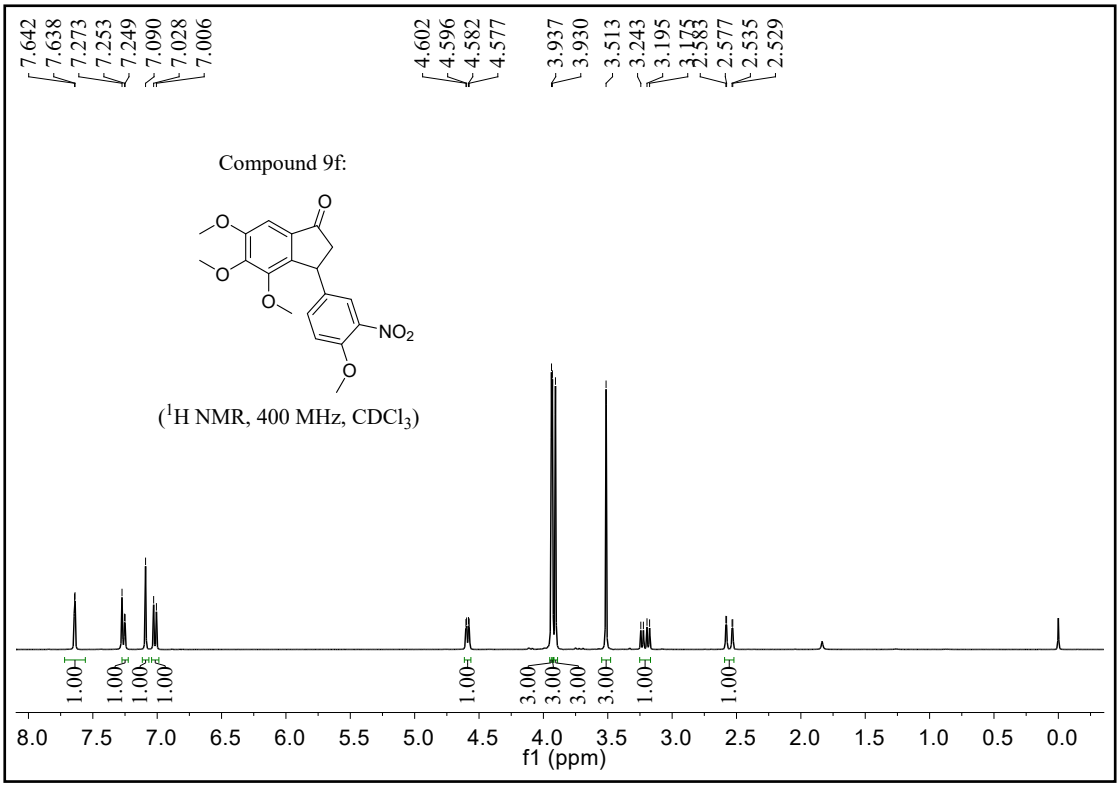

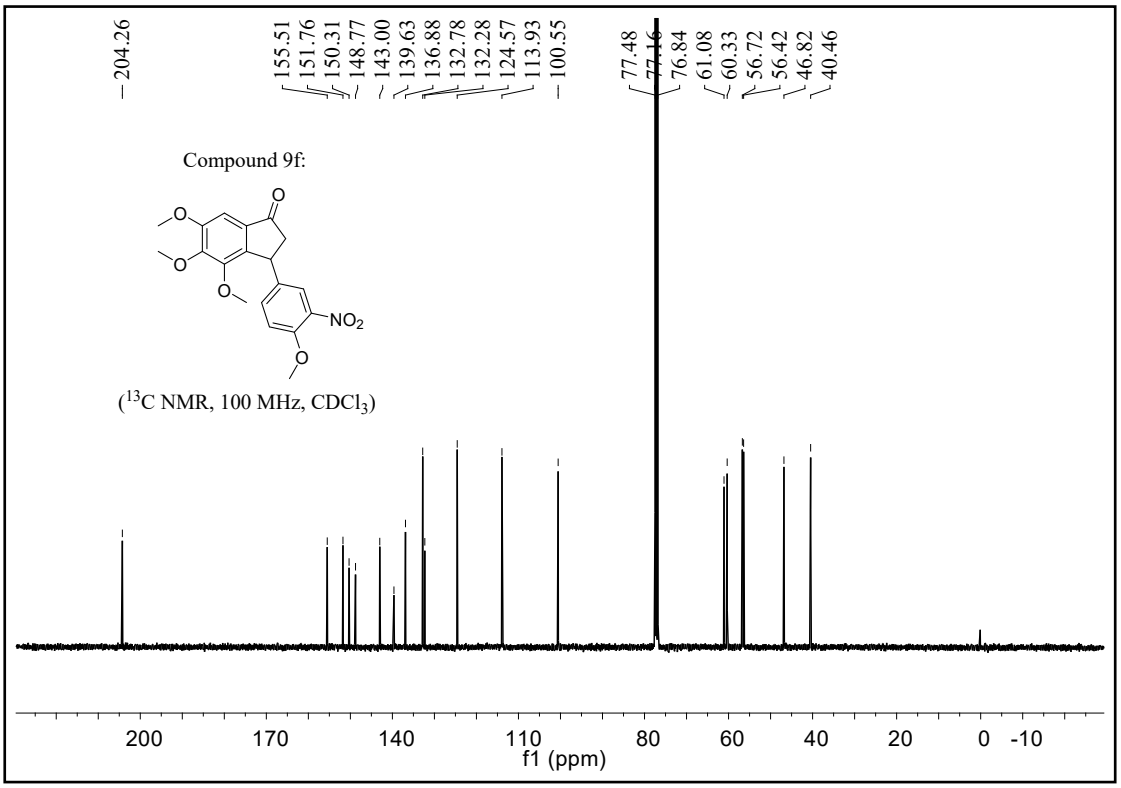
204.26
155.51
151.76
150.31
148.77
143.00
139.63
136.88
132.78
132.28
124.57
113.93
100.55
77.48
77.16
76.84
61.08
60.33
56.72
56.42
46.82
40.46
Compound 9f:
O
O
O
O
NO2
O
(13C NMR, 100 MHz, CDCl3)
200
170
140
110
80
60
40
20
0
-10
f1 (ppm)

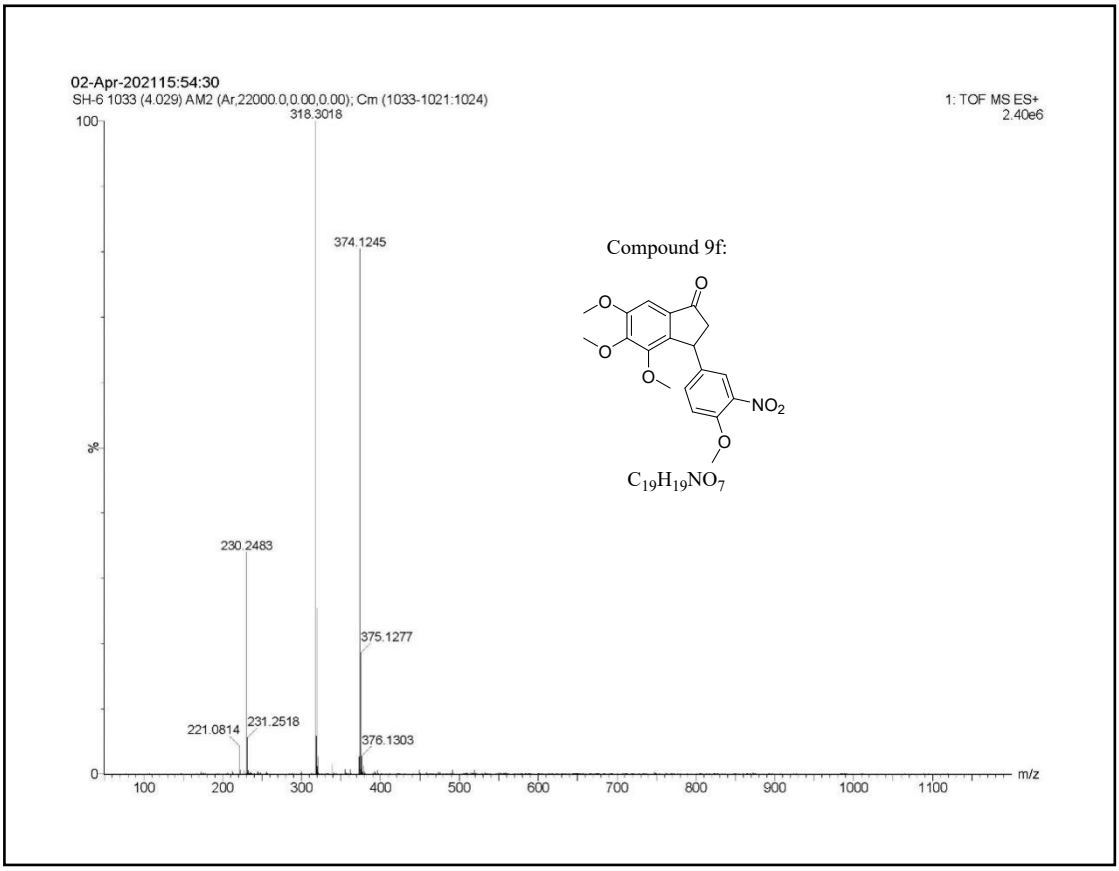
02-Apr-202115:54:30
SH-6 1033 (4.029) AM2 (Ar,22000.0,0.00,0.00); Cm (1033-1021:1024)
1: TOF MS ES+
2.40e6
318.3018
374.1245
230.2483
375.1277
221.0814
231.2518
376.1303
100
%
0
100
200
300
400
500
600
700
800
900
1000
1100
m/z
Compound 9f:
O
O
O
O
NO2
O
C19H19NO7

3-(3,4-Dimethoxyphenyl)-4,5,6-trimethoxy-2,3-dihydro-1H-inden-1-one (**9g**)

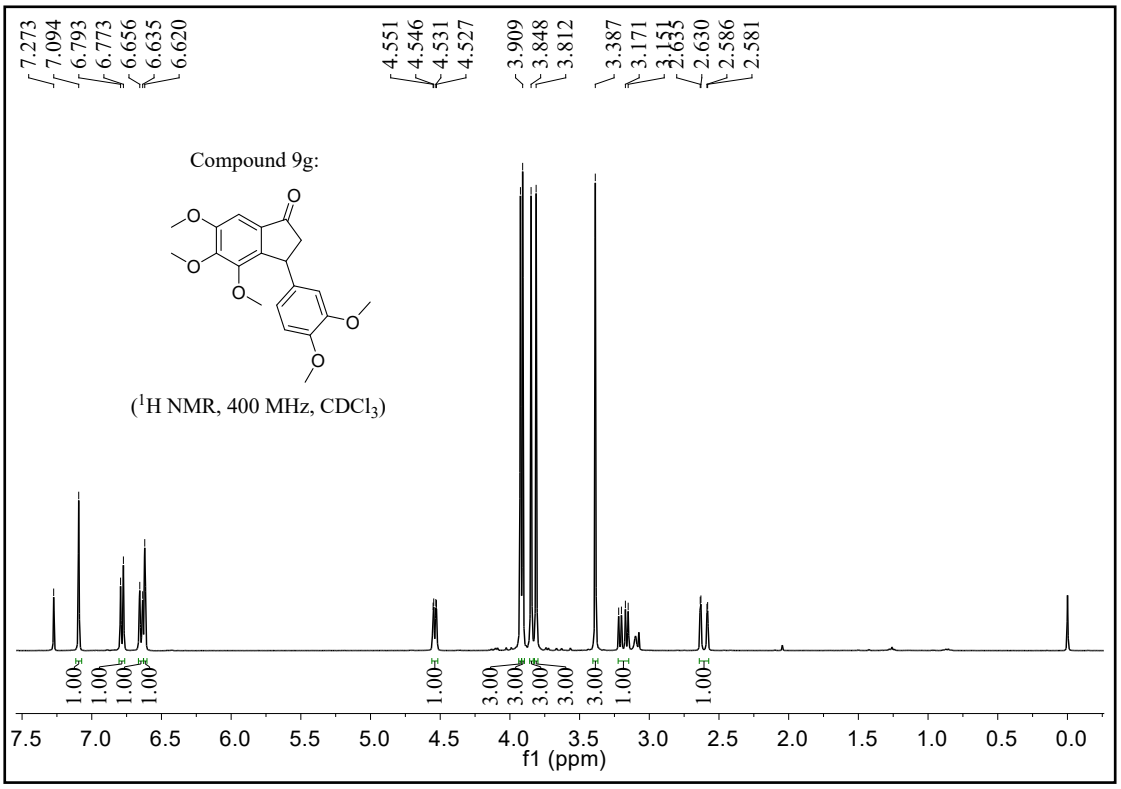

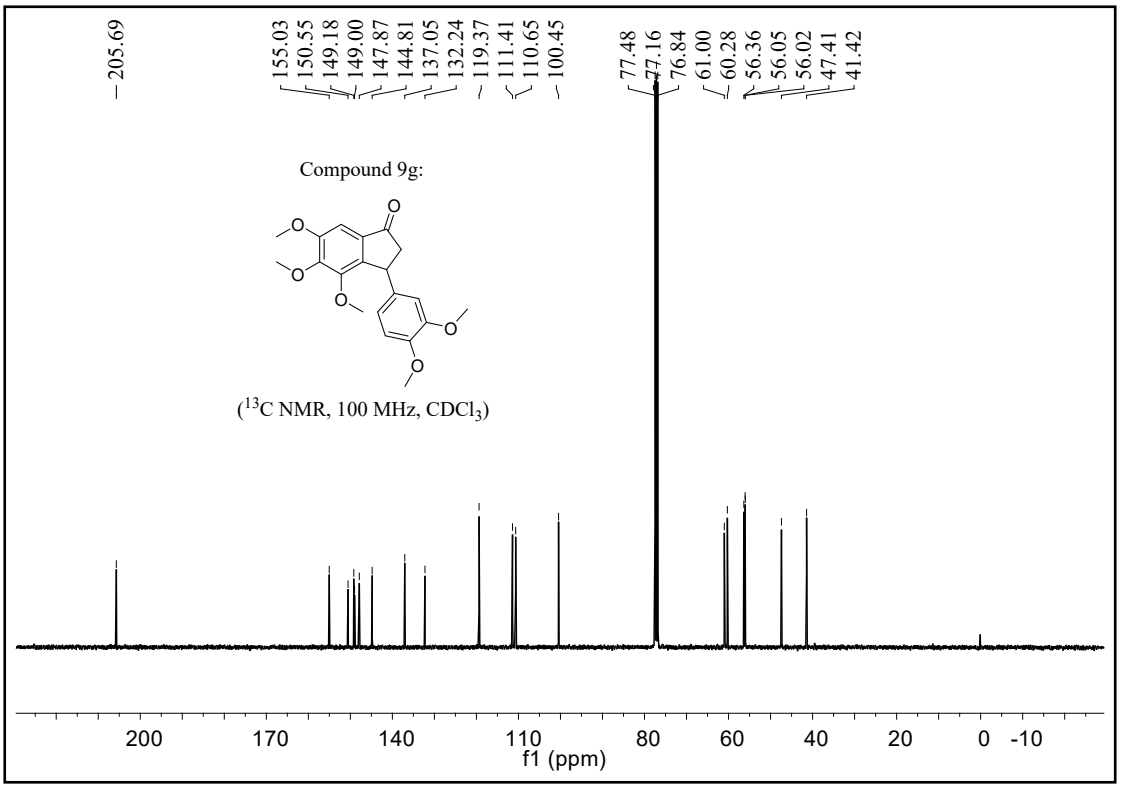

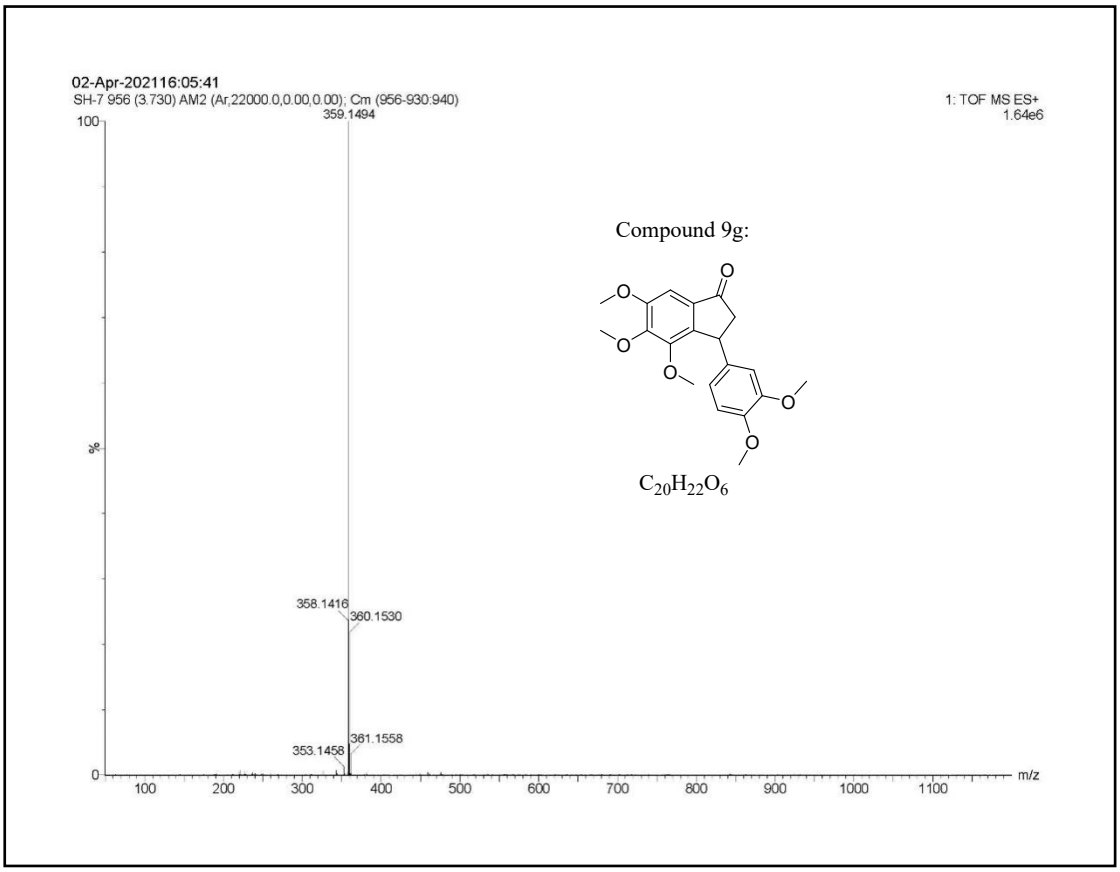

3-(3,5-Dimethoxyphenyl)-4,5,6-trimethoxy-2,3-dihydro-1H-inden-1-one (**9h**)

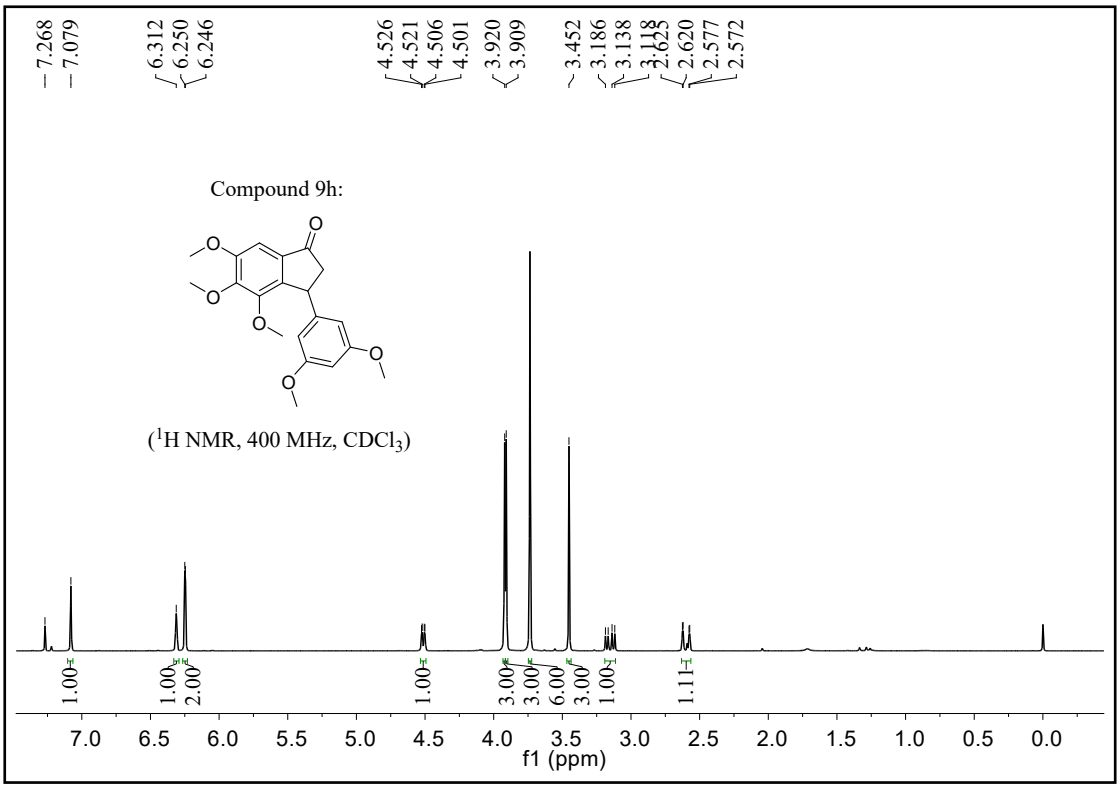

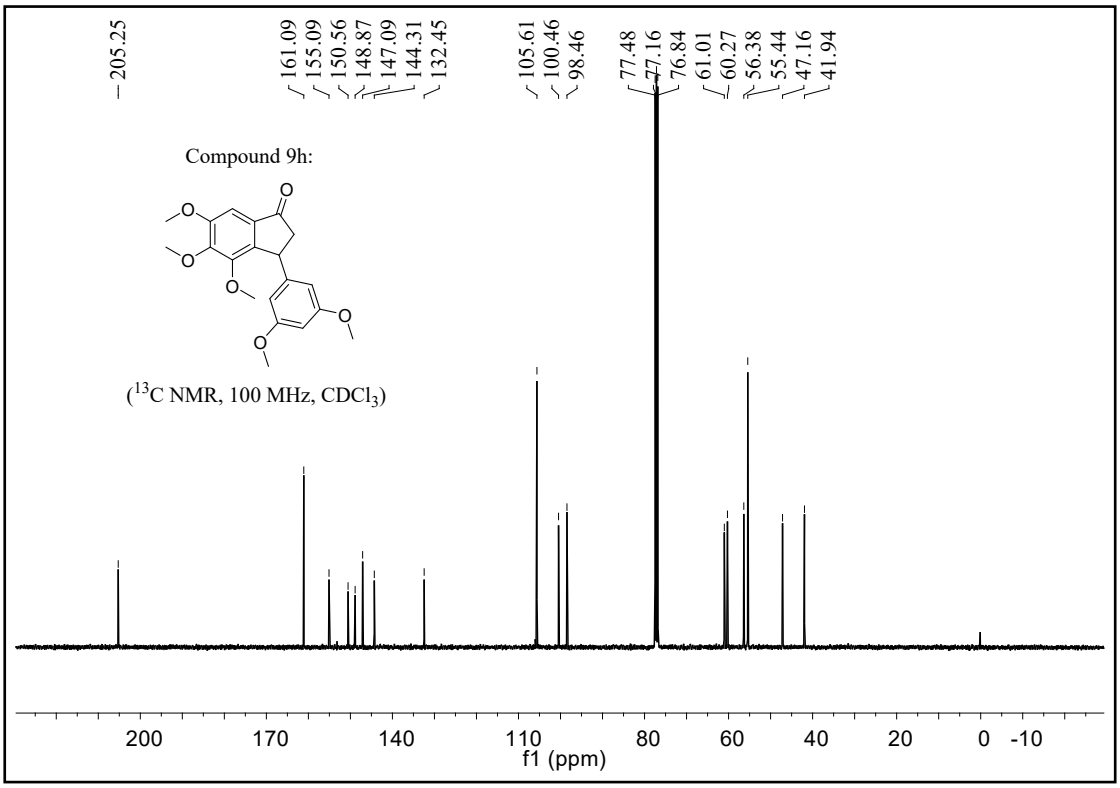
205.25
161.09
155.09
150.56
148.87
147.09
144.31
132.45
105.61
100.46
98.46
77.48
77.16
76.84
61.01
60.27
56.38
55.44
47.16
41.94
Compound 9h:
(^{13}C NMR, 100 MHz, CDCl$_3$)
200
170
140
110
80
60
40
20
0
-10
f1 (ppm)

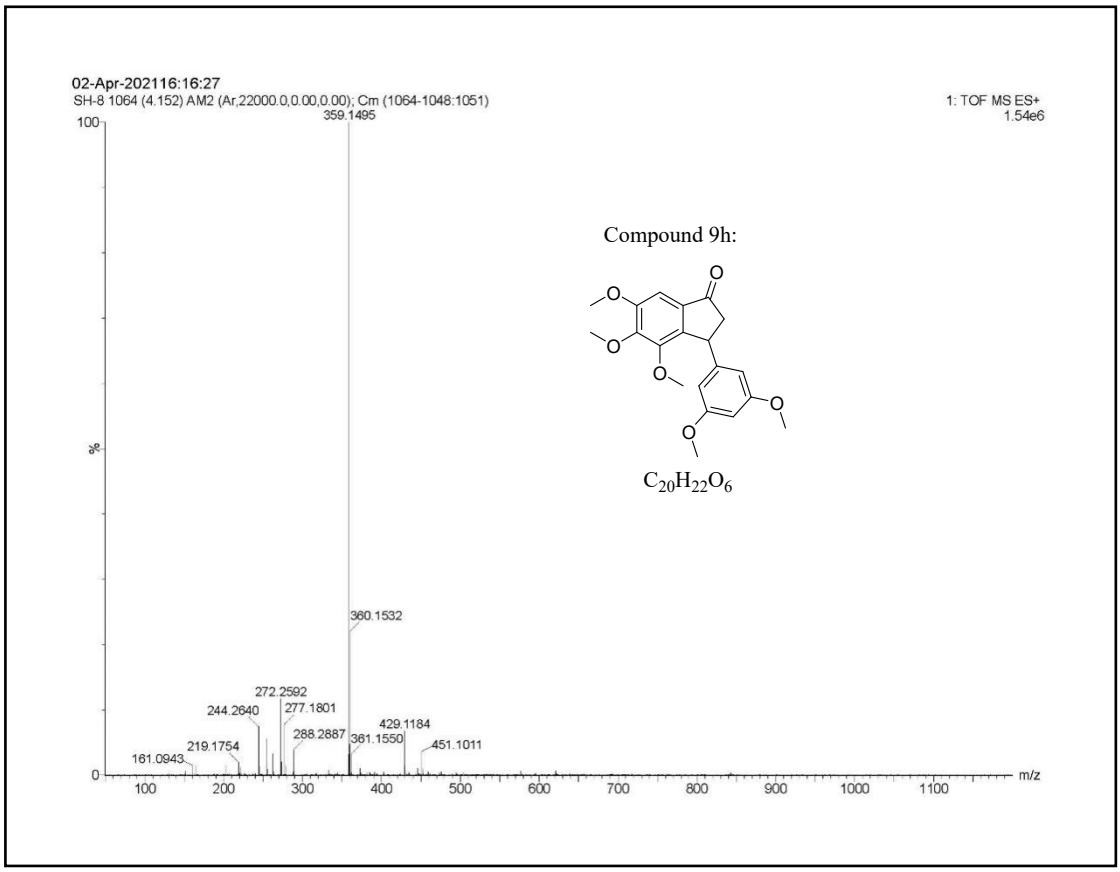
02-Apr-202116:16:27
SH-8 1064 (4.152) AM2 (Ar,22000.0,0.00,0.00); Cm (1064-1048:1051)
1: TOF MS ES+
1.54e6
359.1495
100
%
0
360.1532
272.2592
277.1801
244.2640
288.2887
429.1184
361.1550
451.1011
219.1754
161.0943
100
200
300
400
500
600
700
800
900
1000
1100
m/z
Compound 9h:
C20H22O6

4,5,6-Trimethoxy-3-(3,4,5-trimethoxyphenyl)-2,3-dihydro-1H-inden-1-one (**9i**)

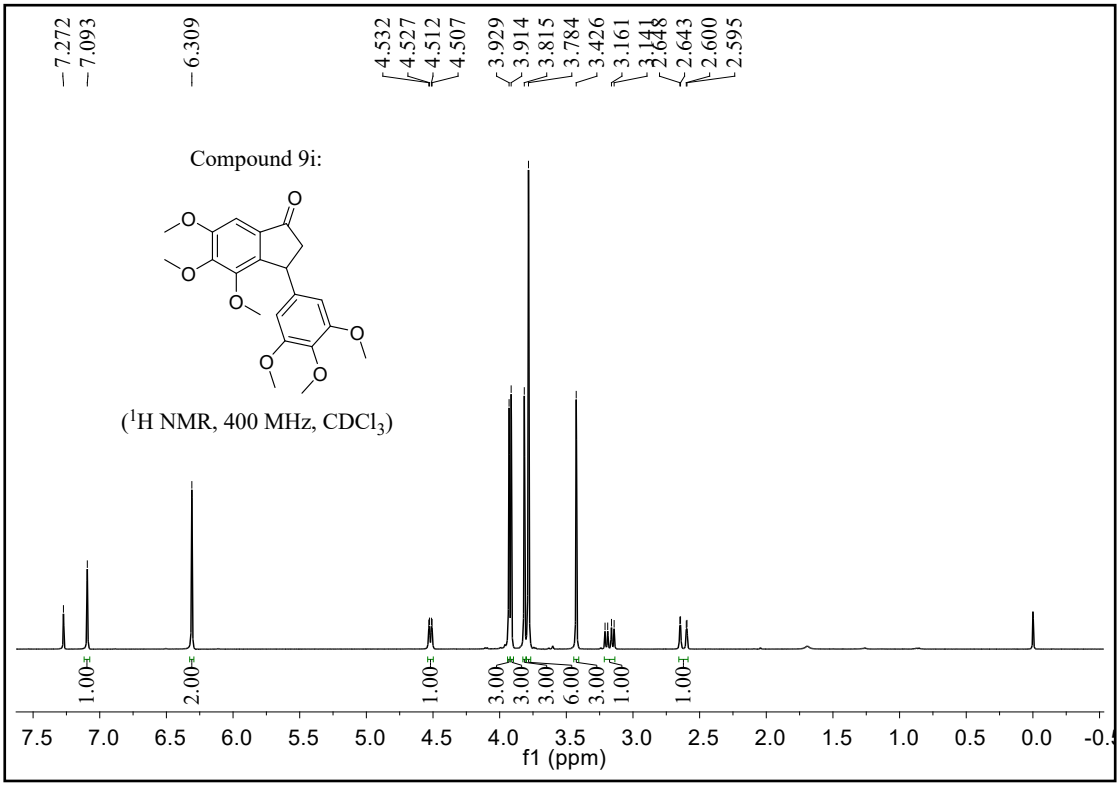

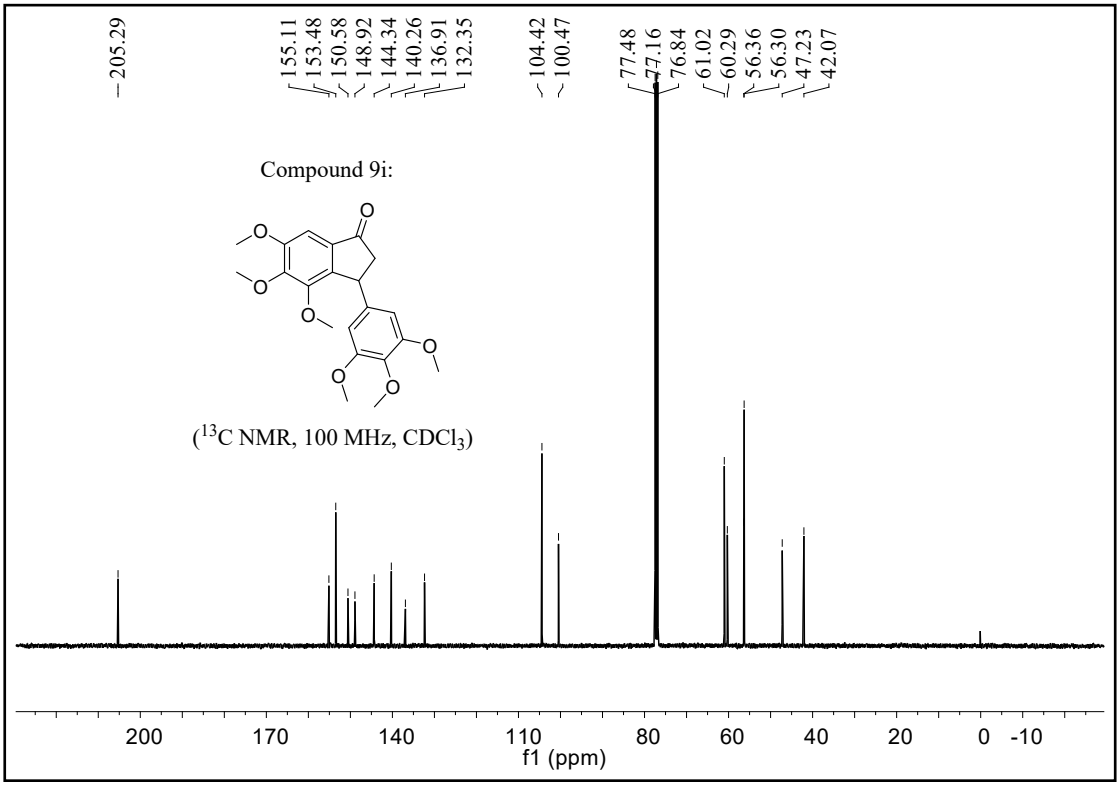

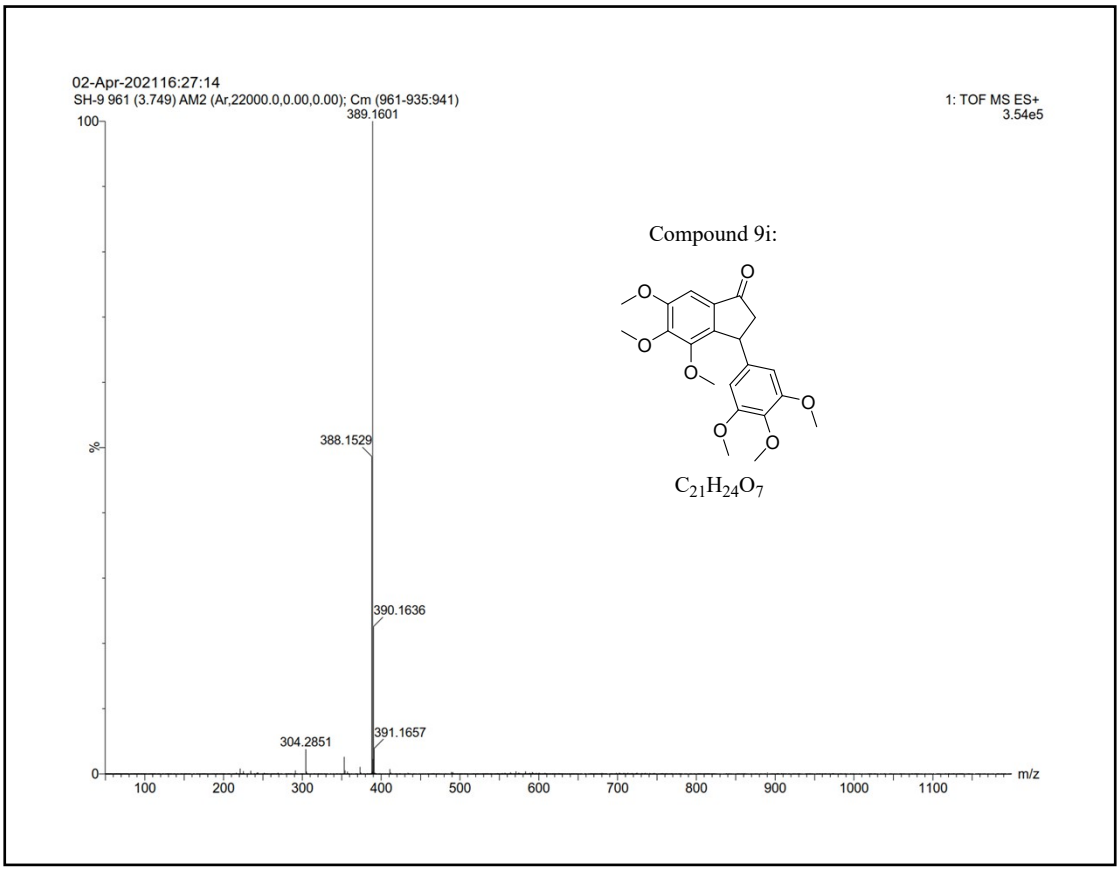

3-(4-Ethoxyphenyl)-4,5,6-trimethoxy-2,3-dihydro-1H-inden-1-one (**9j**)

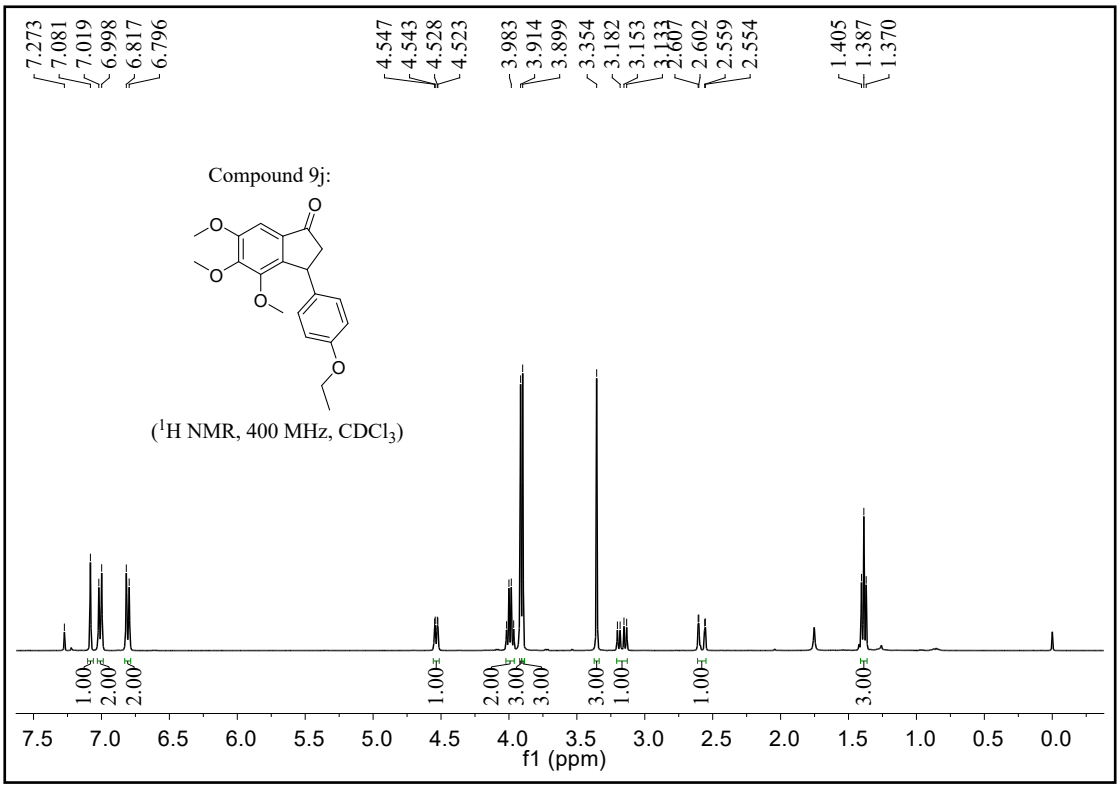

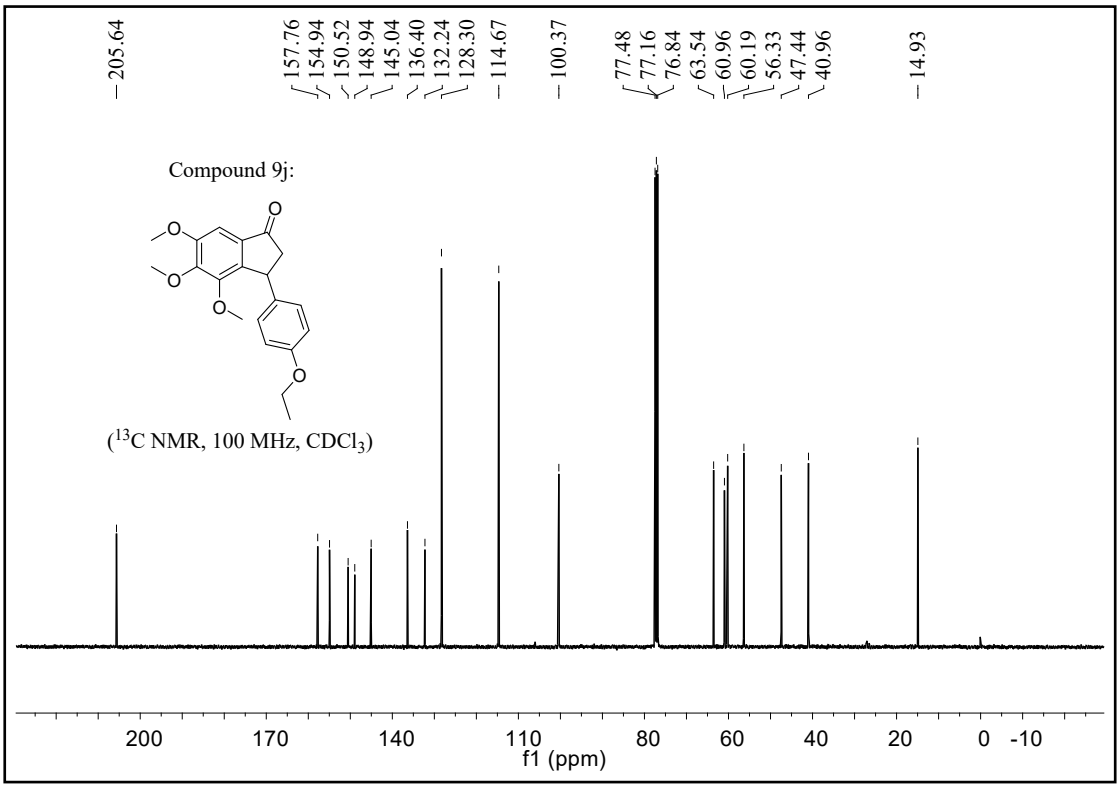
205.64
157.76
154.94
150.52
148.94
145.04
136.40
132.24
128.30
114.67
100.37
77.48
77.16
76.84
63.54
60.96
60.19
56.33
47.44
40.96
14.93
Compound 9j:
(^{13}C NMR, 100 MHz, $CDCl_3$)
200
170
140
110
80
60
40
20
0
-10
f1 (ppm)

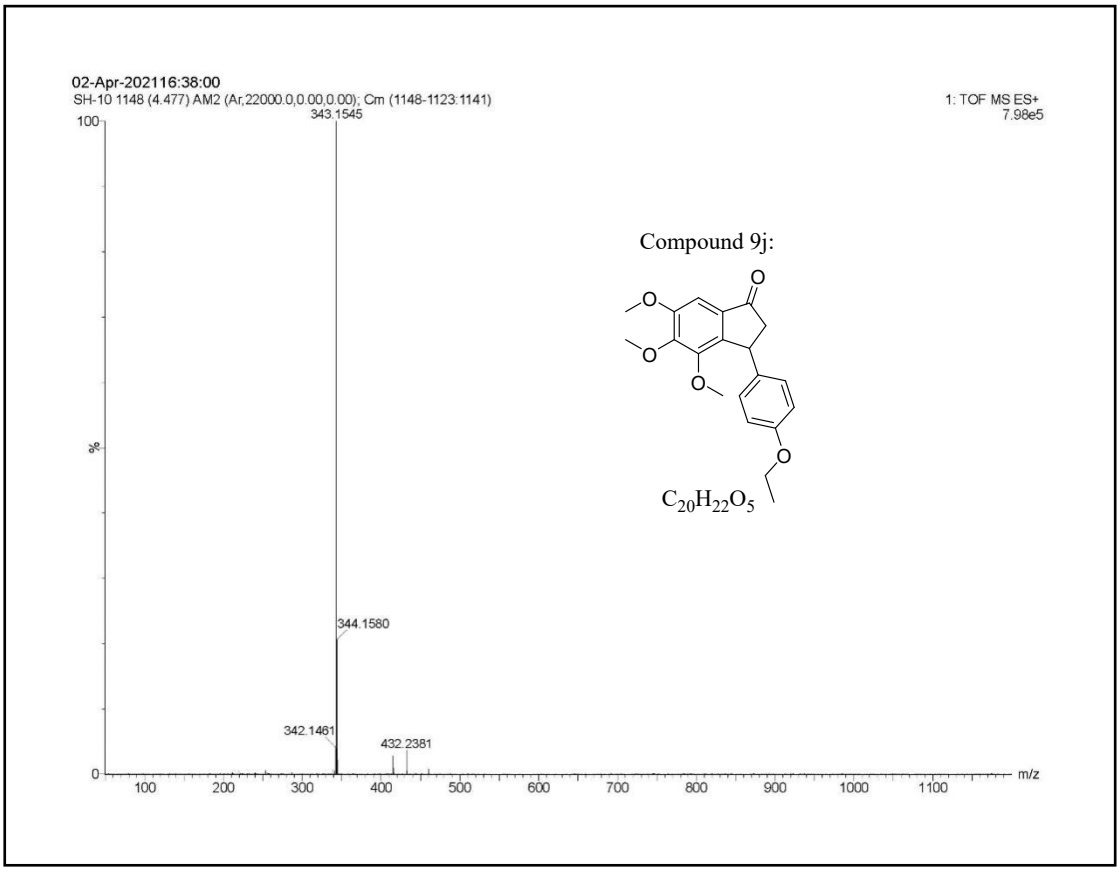
02-Apr-202116:38:00
SH-10 1148 (4.477) AM2 (Ar,22000.0,0.00,0.00); Cm (1148-1123:1141)
1: TOF MS ES+
7.98e5
343.1545
344.1580
342.1461
432.2381
%
m/z
Compound 9j:
$C_{20}H_{22}O_5$

3-(4-Ethoxy-3-fluorophenyl)-4,5,6-trimethoxy-2,3-dihydro-1H-inden-1-one (**9k**)

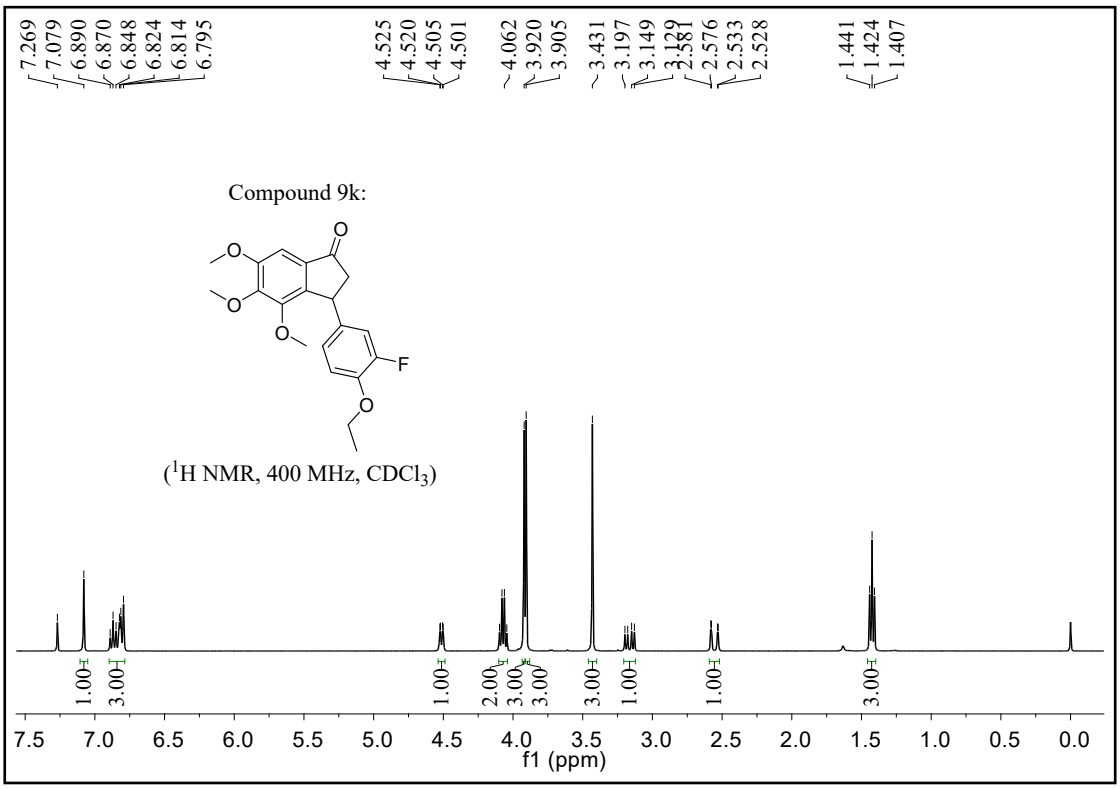

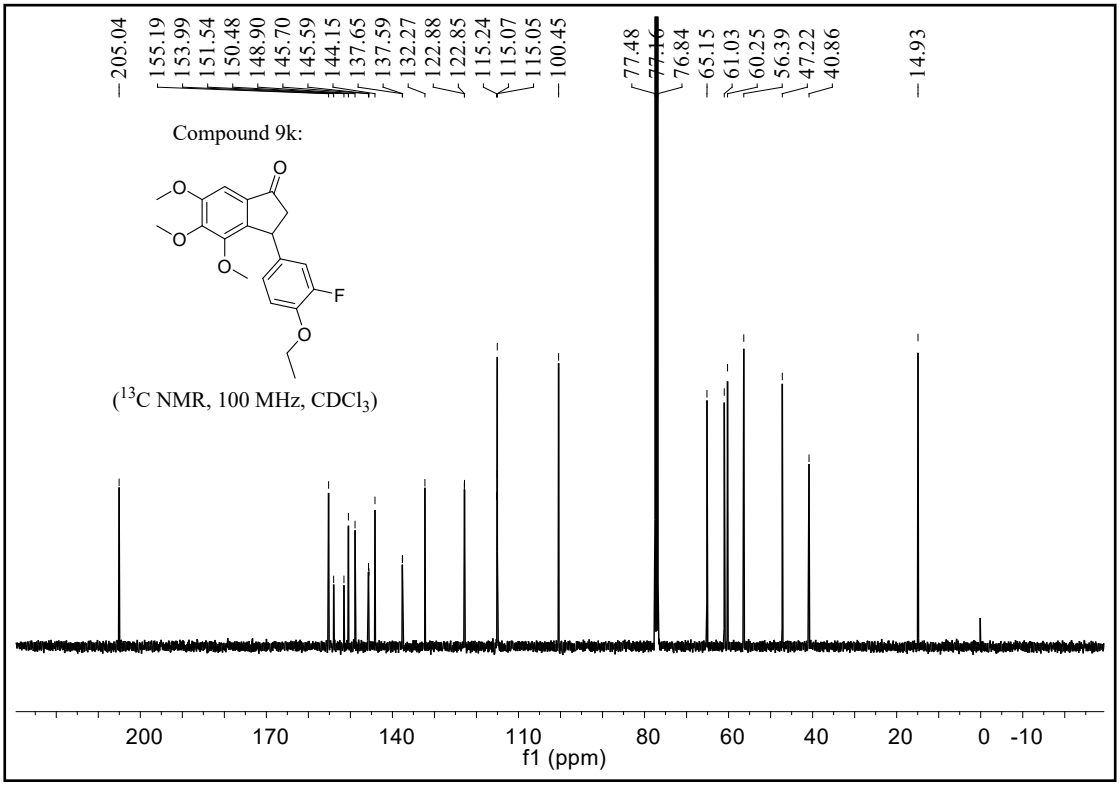

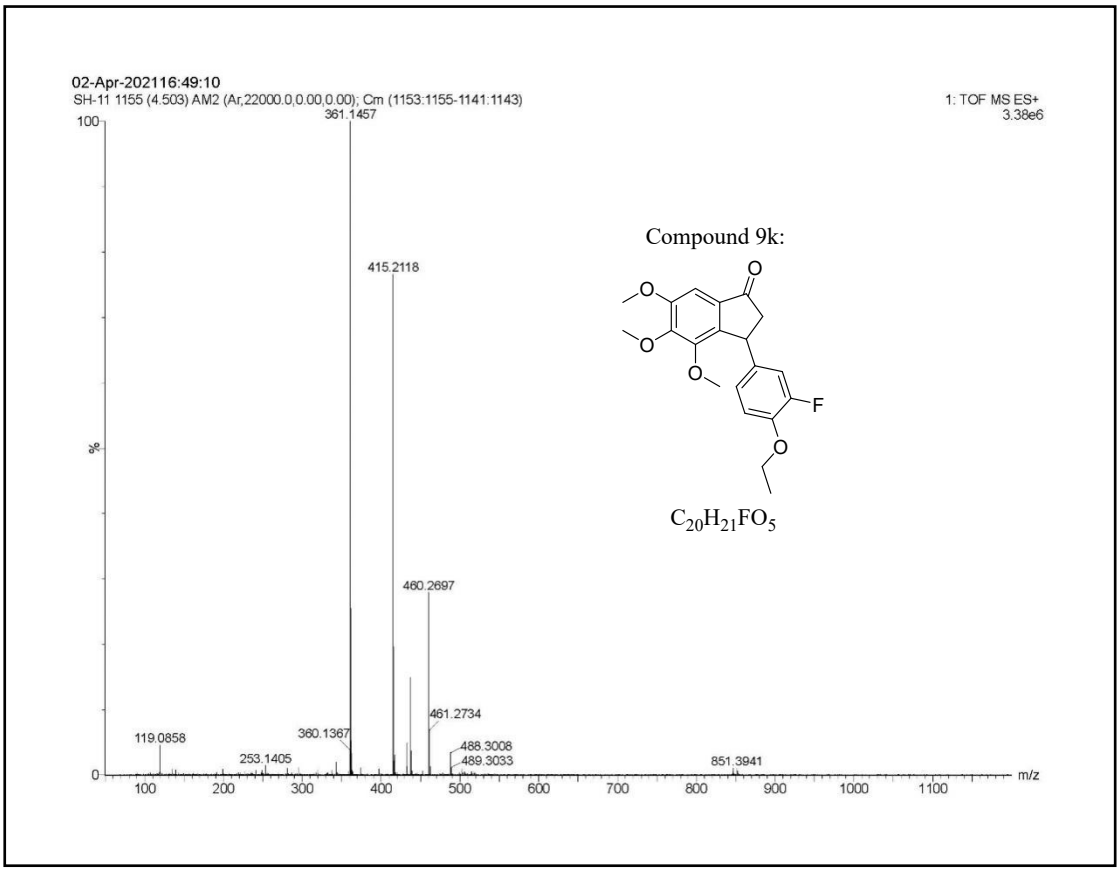

3-(3-Chloro-4-ethoxyphenyl)-4,5,6-trimethoxy-2,3-dihydro-1H-inden-1-one (**9l**)

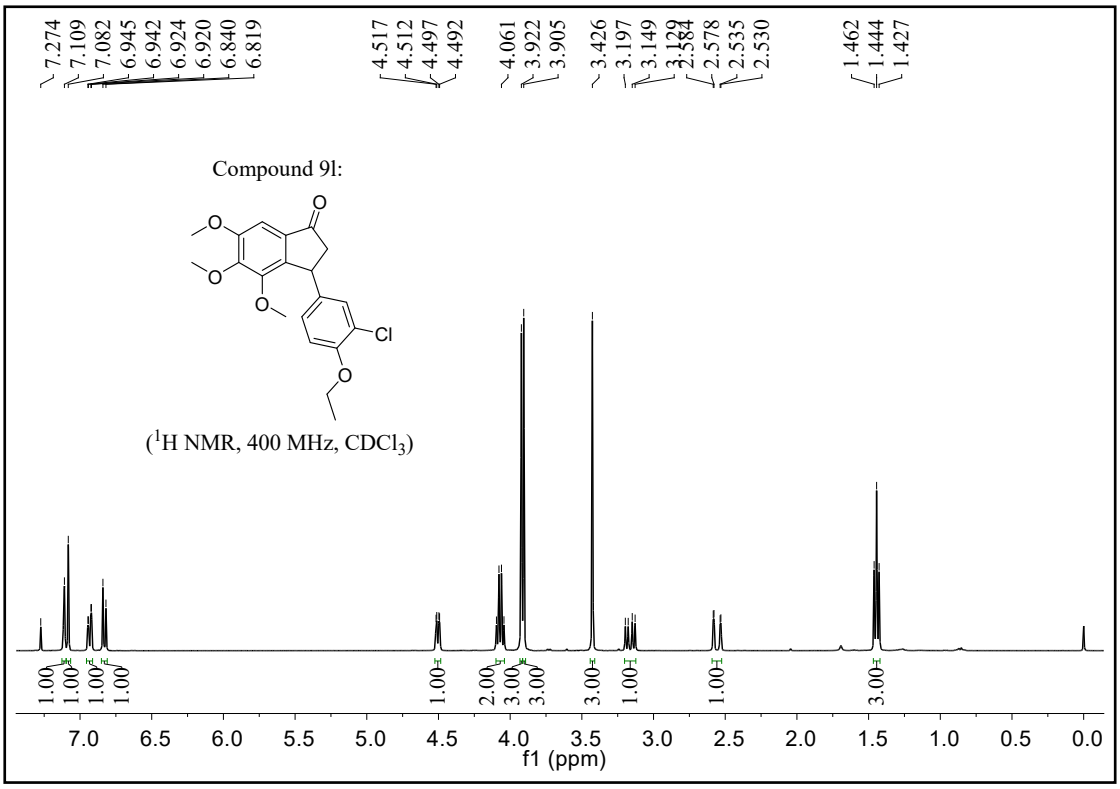

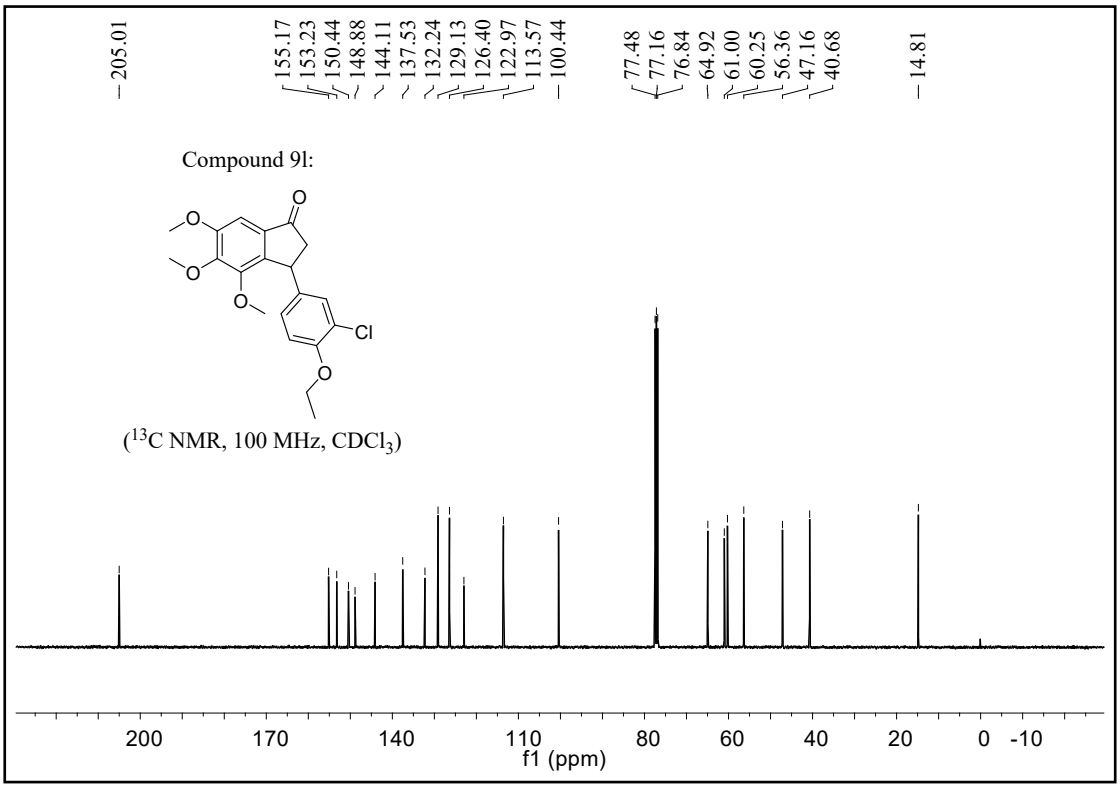
205.01
155.17
153.23
150.44
148.88
144.11
137.53
132.24
129.13
126.40
122.97
113.57
100.44
77.48
77.16
76.84
64.92
61.00
60.25
56.36
47.16
40.68
14.81
Compound 9l:
O
O
O
O
Cl
O
(^{13}C NMR, 100 MHz, $CDCl_3$)
200
170
140
110
80
60
40
20
0
-10
f1 (ppm)

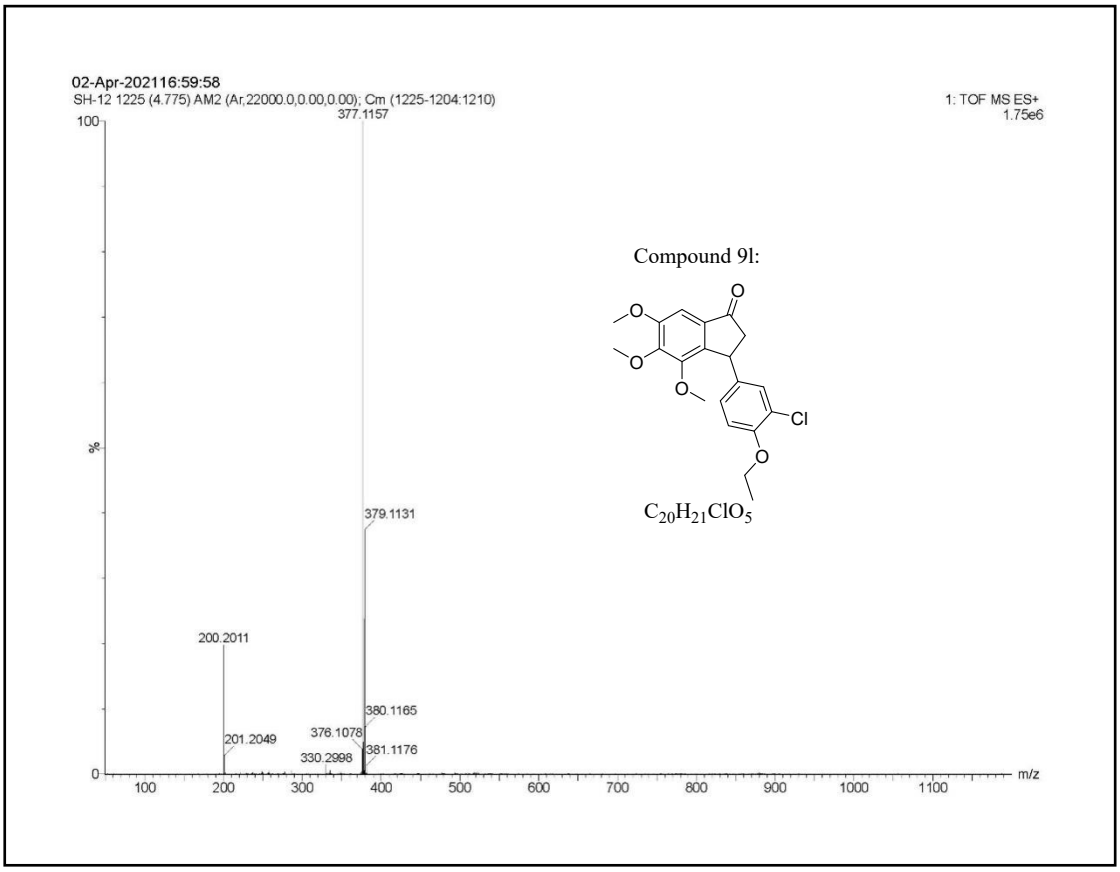
02-Apr-202116:59:58
SH-12 1225 (4.775) AM2 (Ar,22000.0,0.00,0.00); Cm (1225-1204:1210)
1: TOF MS ES+
1.75e6
377.1157
379.1131
200.2011
380.1165
376.1078
201.2049
330.2998
381.1176
100
%
0
100
200
300
400
500
600
700
800
900
1000
1100
m/z
Compound 9l:
O
O
O
O
Cl
O
$C_{20}H_{21}ClO_5$

3-(3-Bromo-4-ethoxyphenyl)-4,5,6-trimethoxy-2,3-dihydro-1H-inden-1-one (**9m**)

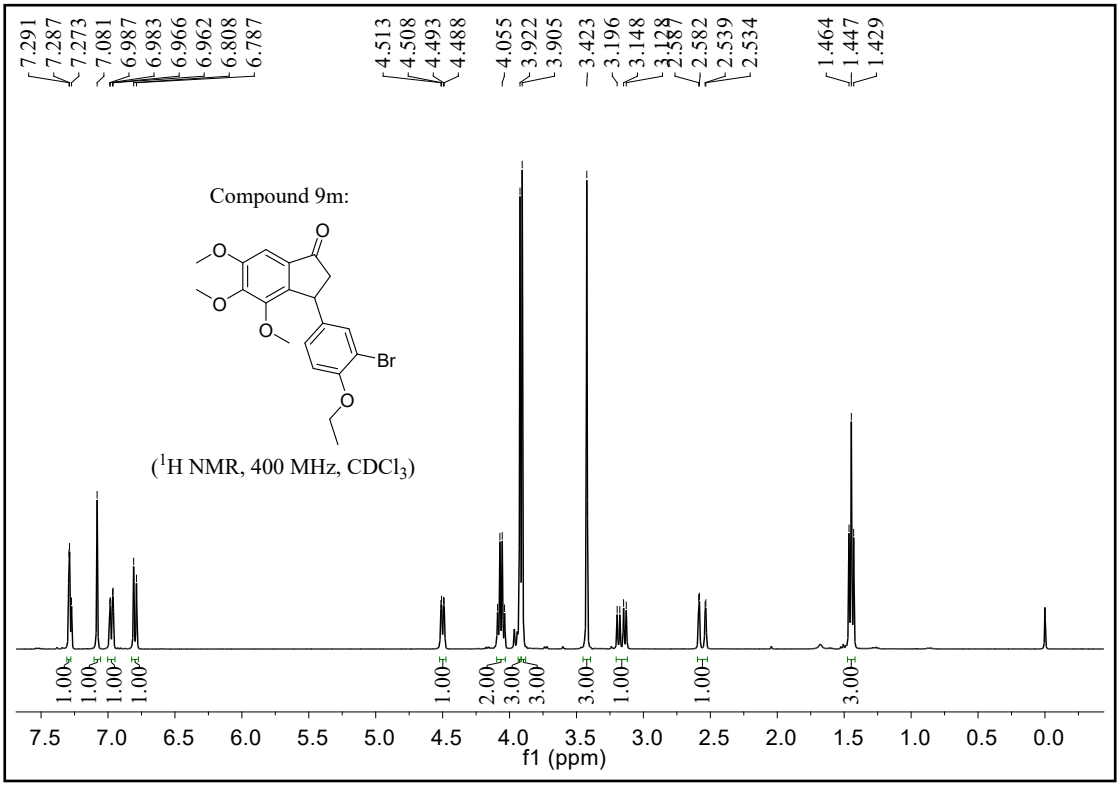

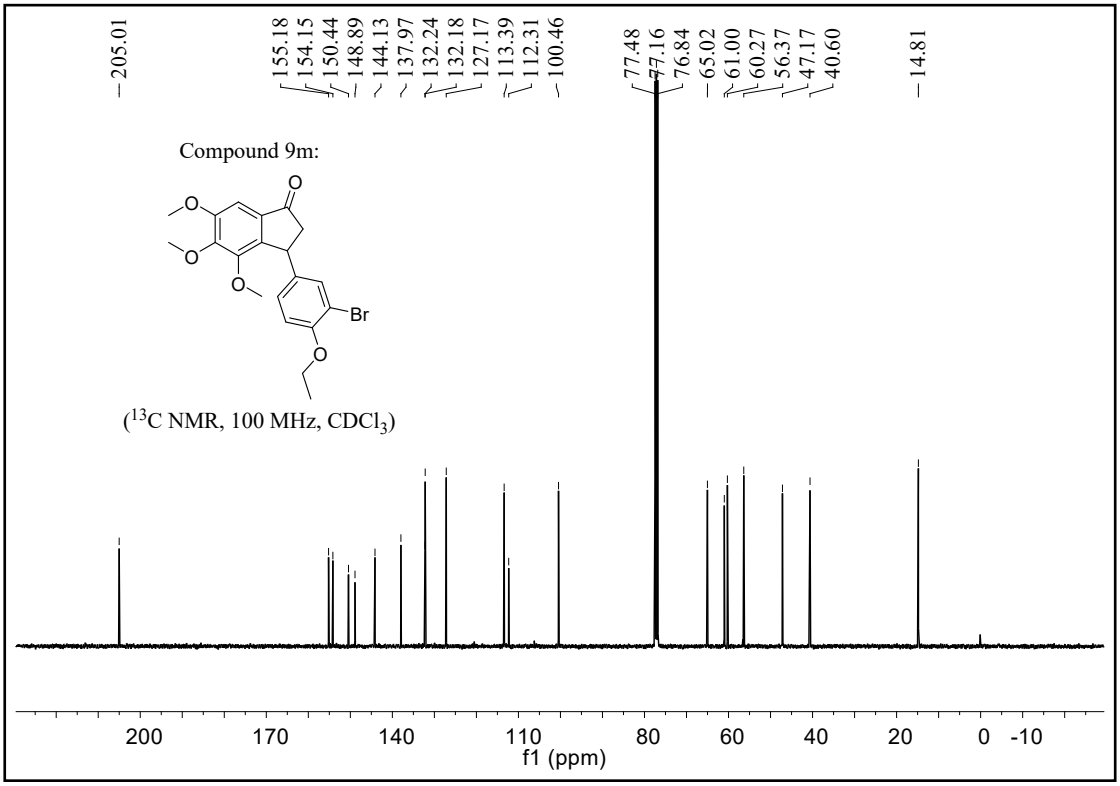

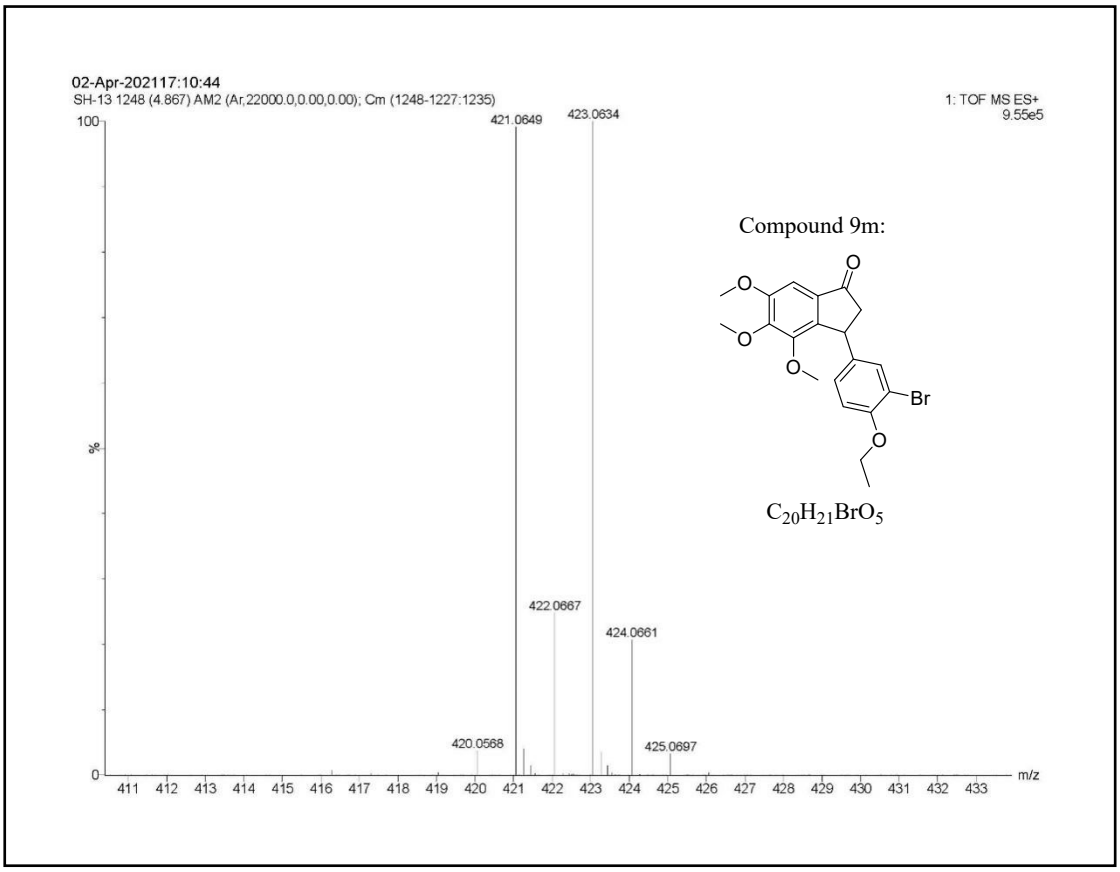

3-(4-Isopropoxyphenyl)-4,5,6-trimethoxy-2,3-dihydro-1H-inden-1-one (**9n**)

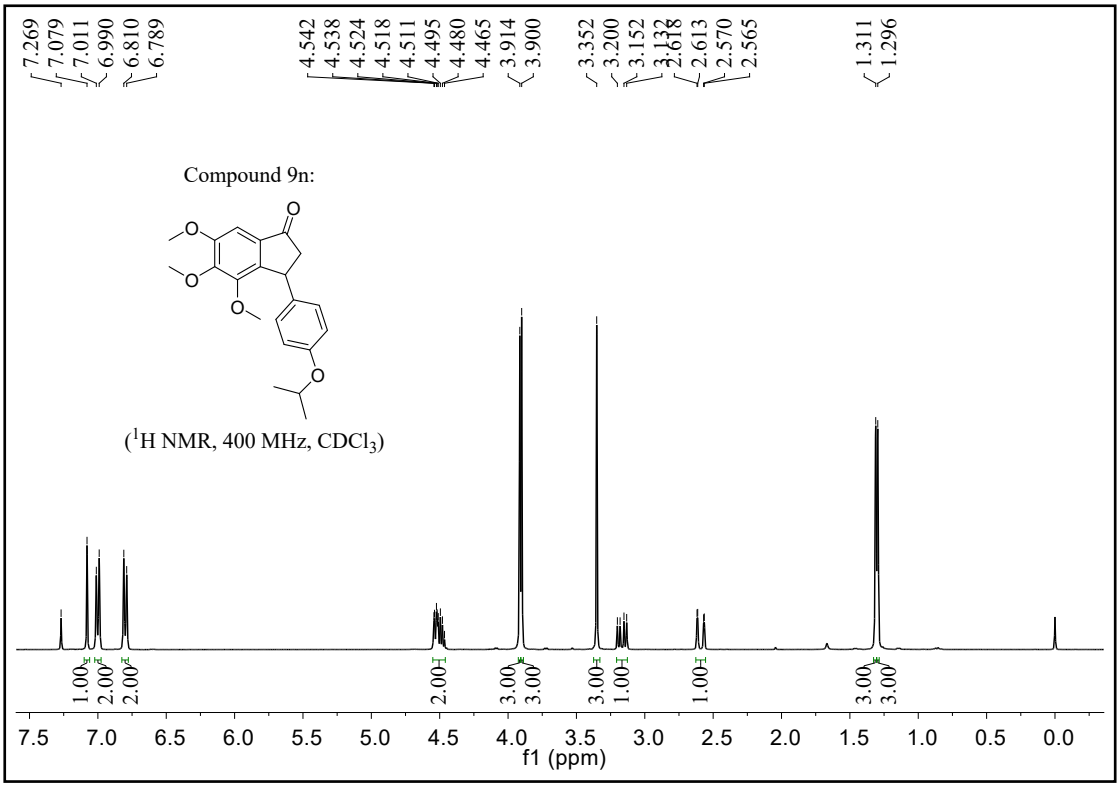

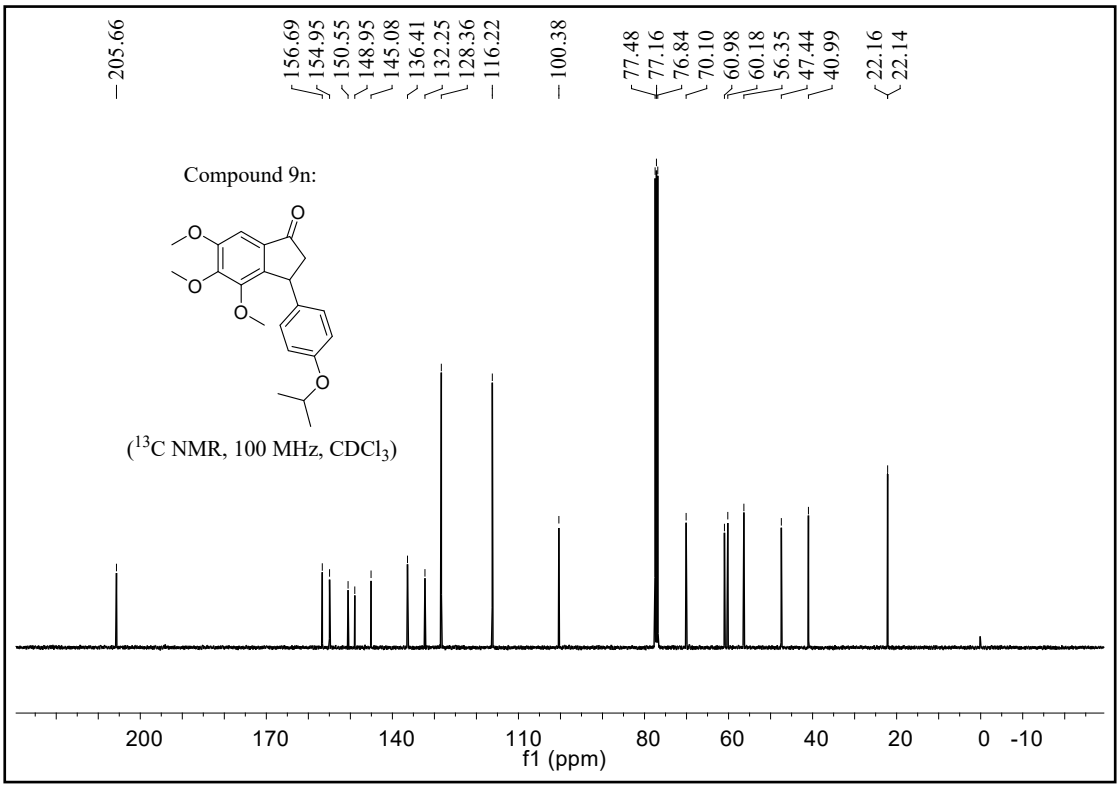
205.66
156.69
154.95
150.55
148.95
145.08
136.41
132.25
128.36
116.22
100.38
77.48
77.16
76.84
70.10
60.98
60.18
56.35
47.44
40.99
22.16
22.14
Compound 9n:
(^{13}C NMR, 100 MHz, $CDCl_3$)
200
170
140
110
80
60
40
20
0
-10
f1 (ppm)

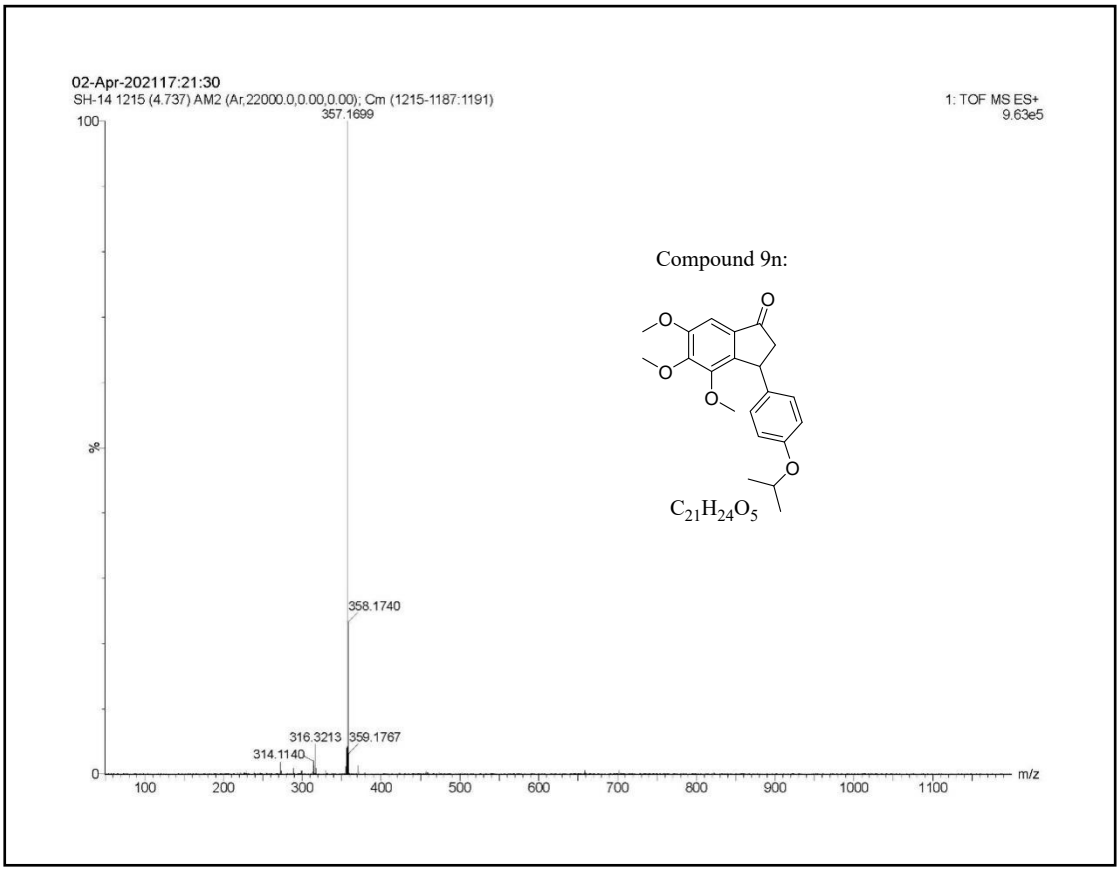
02-Apr-202117:21:30
SH-14 1215 (4.737) AM2 (Ar,22000.0,0.00,0.00); Cm (1215-1187:1191)
1: TOF MS ES+
9.63e5
357.1699
358.1740
316.3213
359.1767
314.1140
%
m/z
Compound 9n:
$C_{21}H_{24}O_5$

3-(4-(tert-Butoxy)phenyl)-4,5,6-trimethoxy-2,3-dihydro-1H-inden-1-one (**9o**)

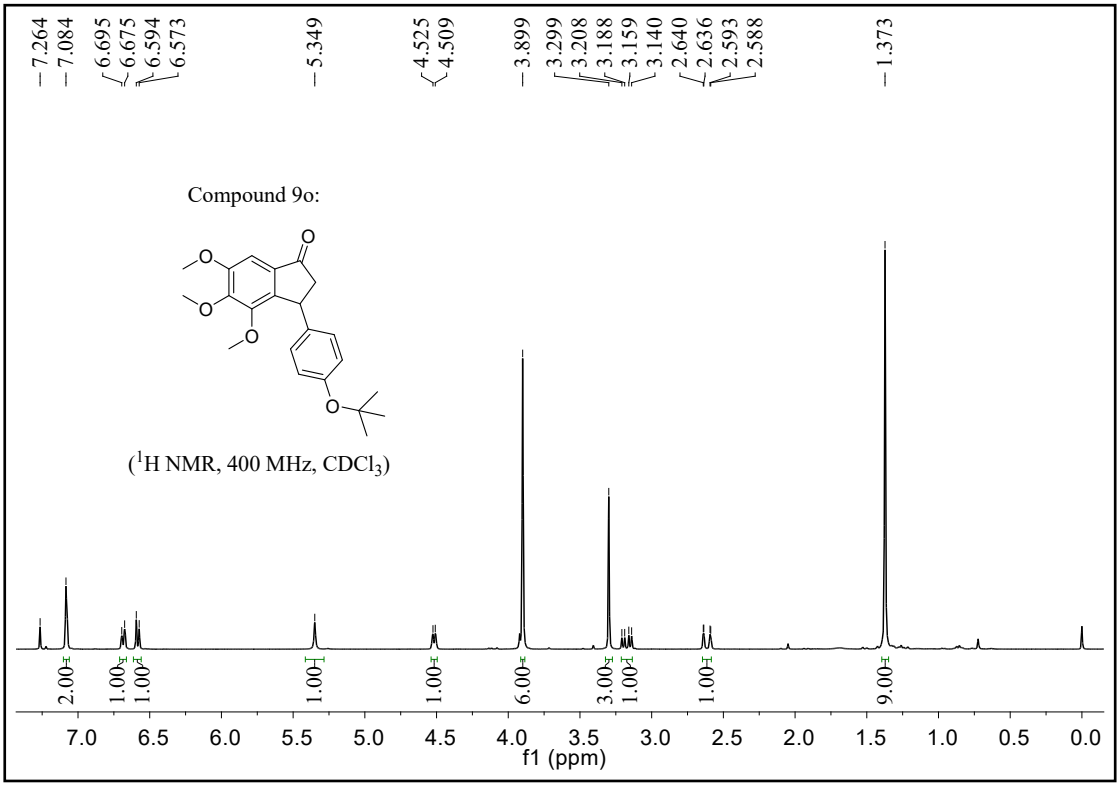

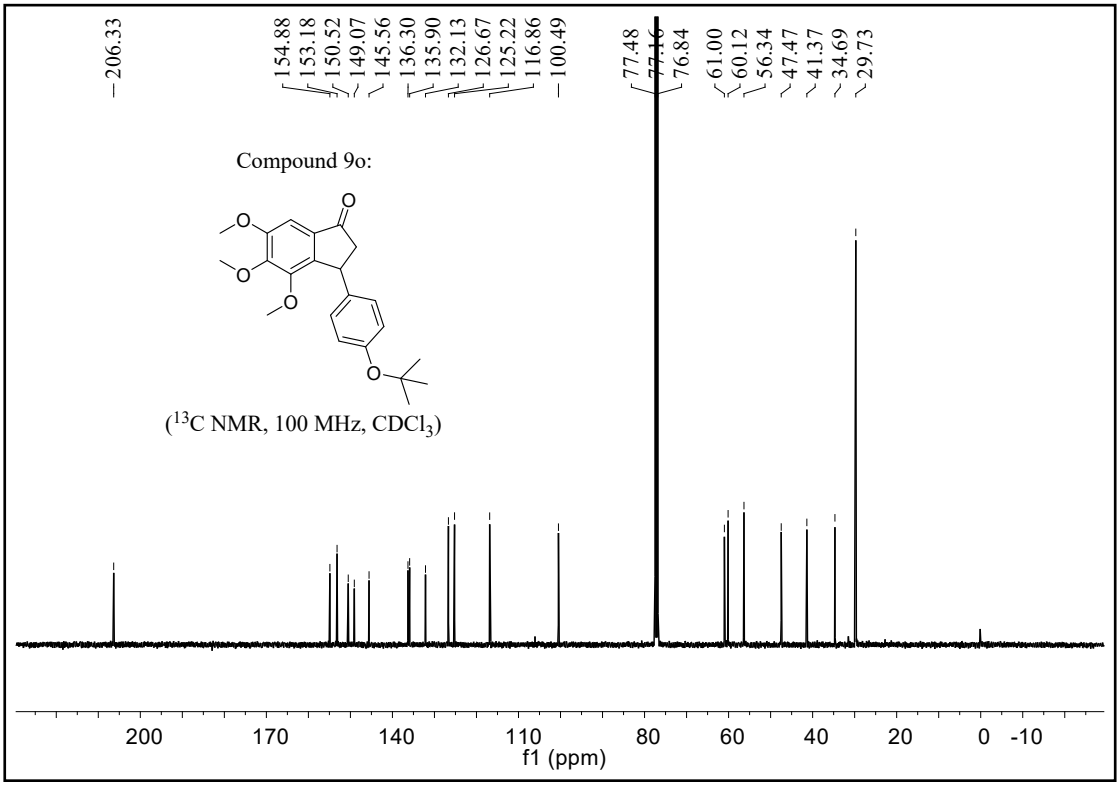

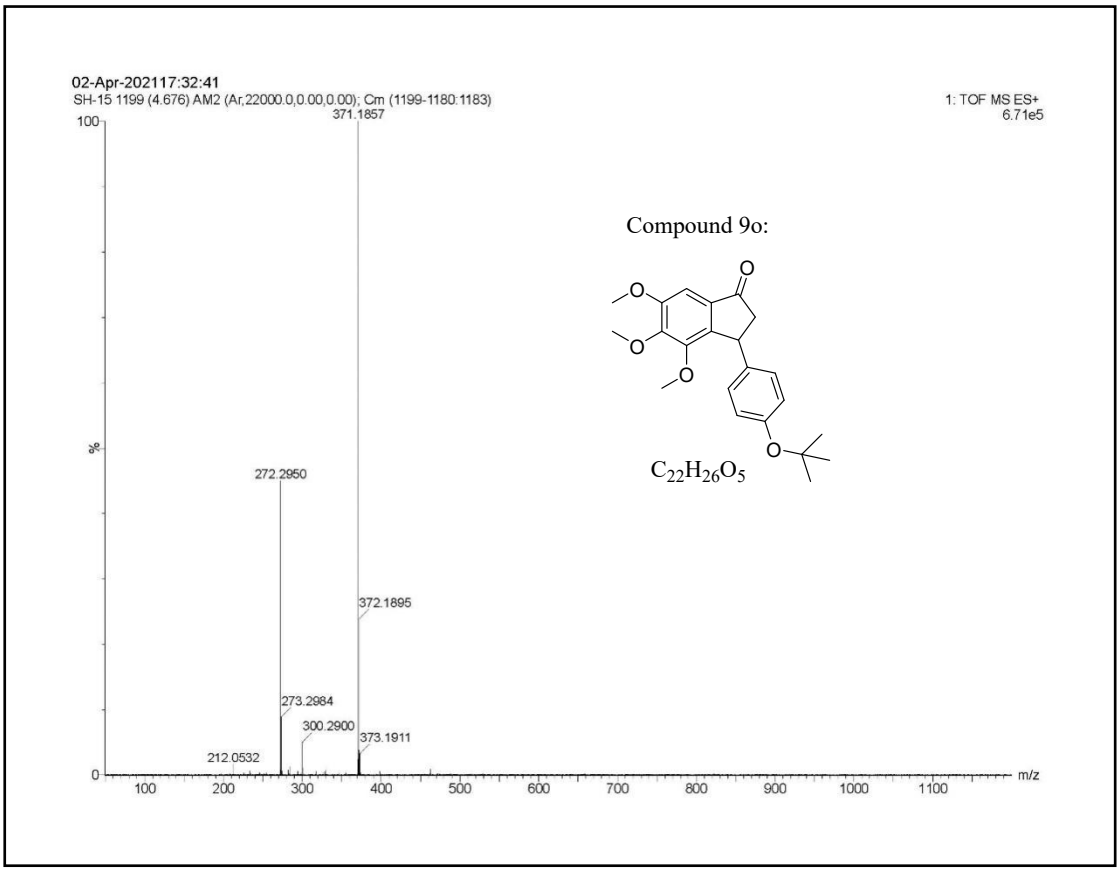

4,5,6-Trimethoxy-3-(4-(methylthio)phenyl)-2,3-dihydro-1H-inden-1-one (**9p**)

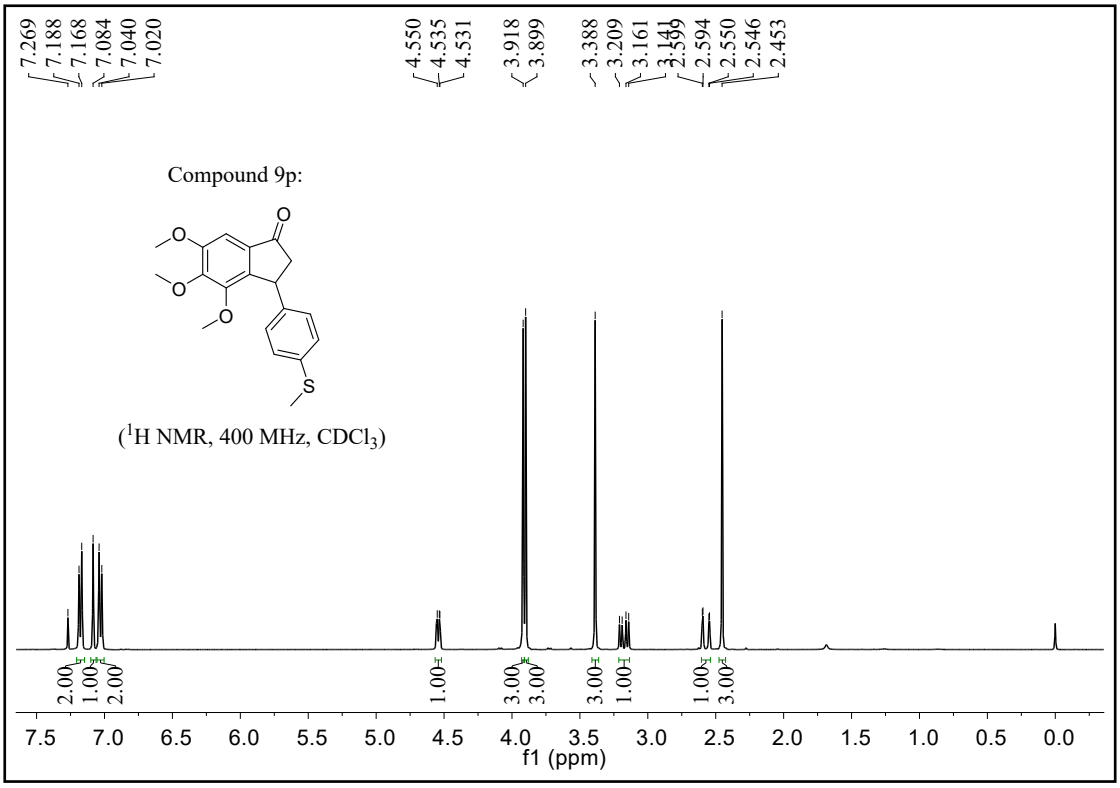

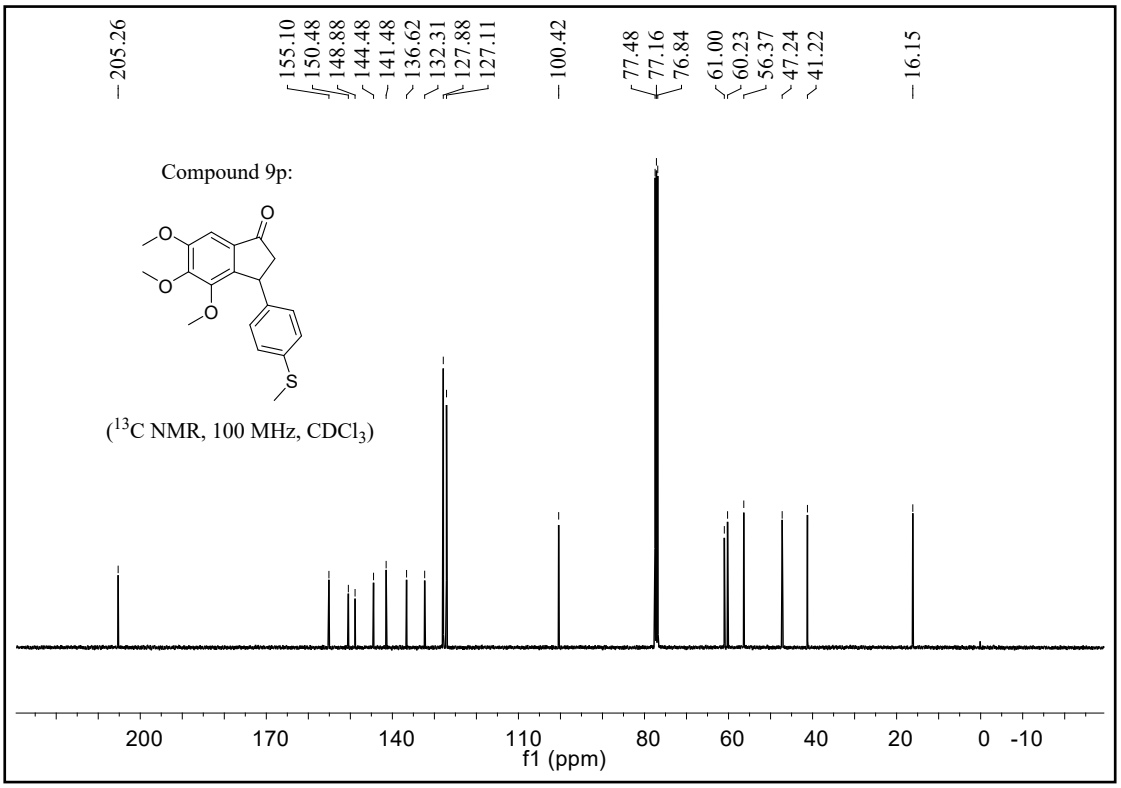
205.26
155.10
150.48
148.88
144.48
141.48
136.62
132.31
127.88
127.11
100.42
77.48
77.16
76.84
61.00
60.23
56.37
47.24
41.22
16.15
Compound 9p:
(^{13}C NMR, 100 MHz, $CDCl_3$)
200
170
140
110
80
60
40
20
0
-10
f1 (ppm)

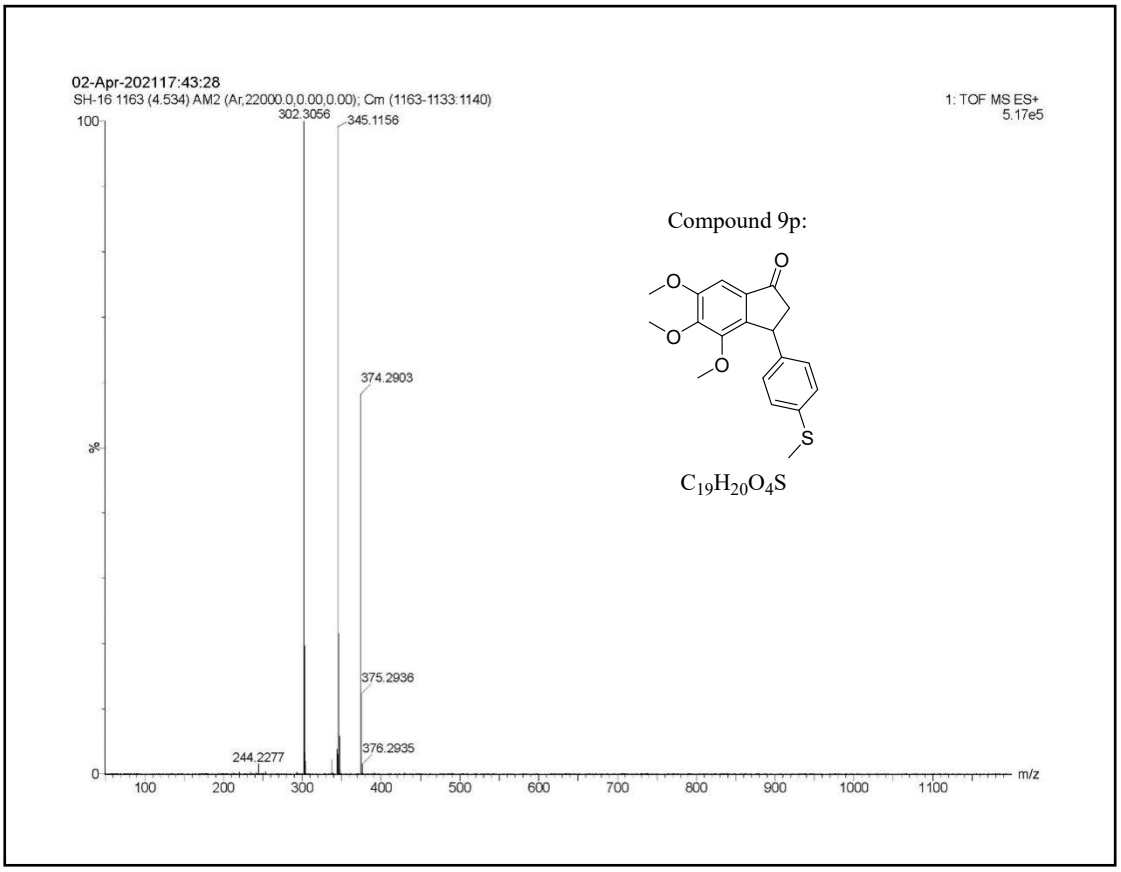
02-Apr-202117:43:28
SH-16 1163 (4.534) AM2 (Ar,22000.0,0.00,0.00); Cm (1163-1133:1140)
1: TOF MS ES+
5.17e5
302.3056
345.1156
374.2903
375.2936
376.2935
244.2277
%
m/z
Compound 9p:
$C_{19}H_{20}O_4S$

3-(4-Chloro-3-methoxyphenyl)-4,5,6-trimethoxy-2,3-dihydro-1H-inden-1-one (**9q**)

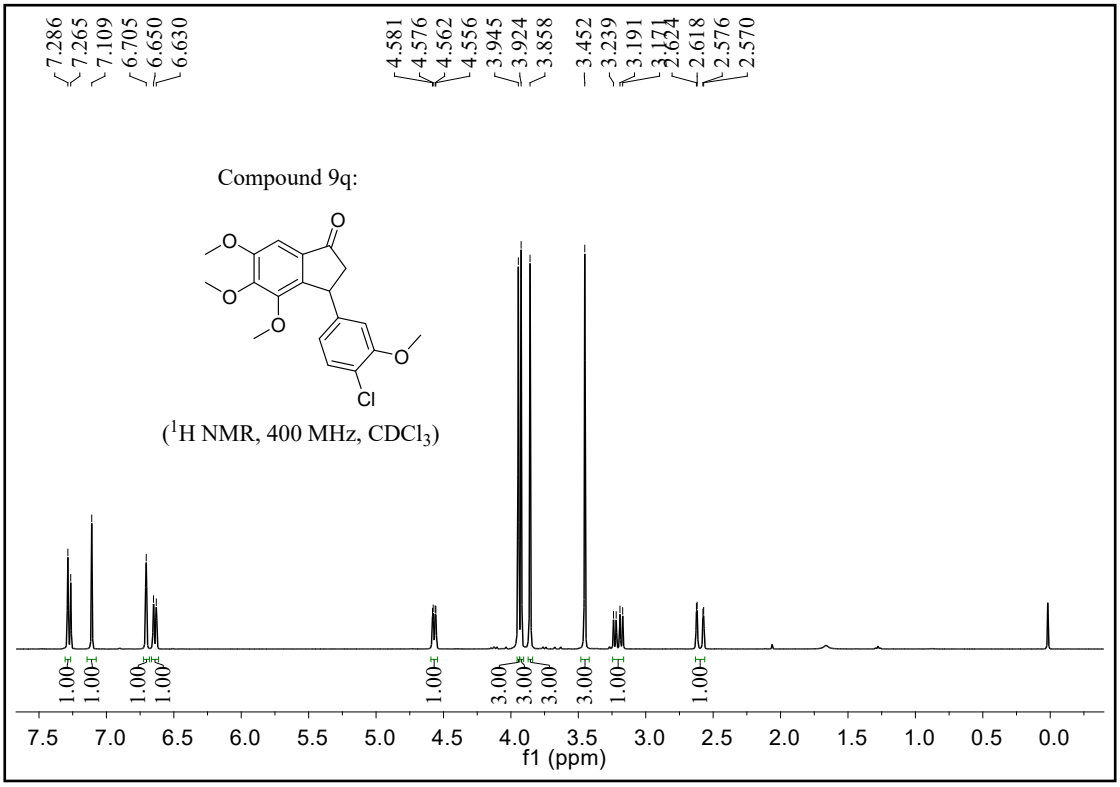

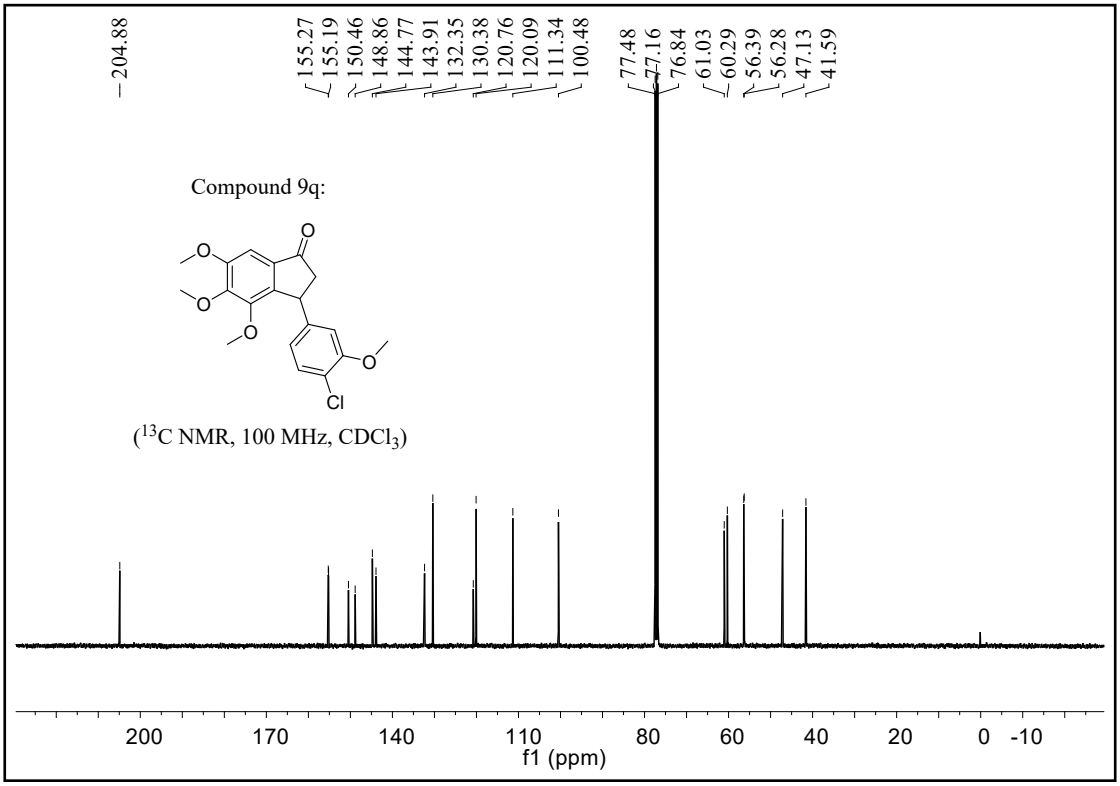

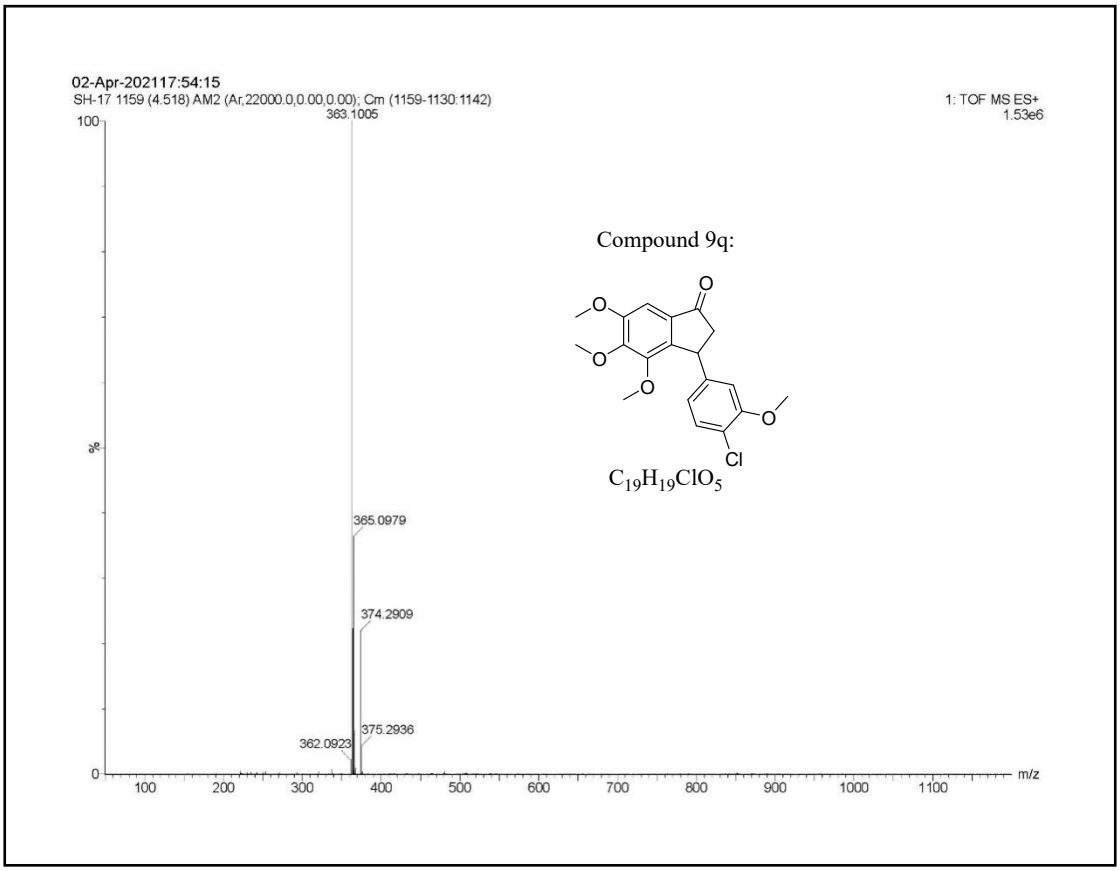
02-Apr-202117:54:15
SH-17 1159 (4.518) AM2 (Ar,22000.0,0.00,0.00); Cm (1159-1130:1142)
1: TOF MS ES+
1.53e6
363.1005
100
%
0
365.0979
374.2909
375.2936
362.0923
100
200
300
400
500
600
700
800
900
1000
1100
m/z
Compound 9q:
O
O
O
O
O
Cl
$C_{19}H_{19}ClO_5$

Compounds **11** and **13** were fully characterized by ^{1}H NMR and ^{13}C NMR.

2-((*R*)-p-methylsulfoxide)-1-(3,4,5-trimethoxyphenyl)ethan-1-one (**11**)

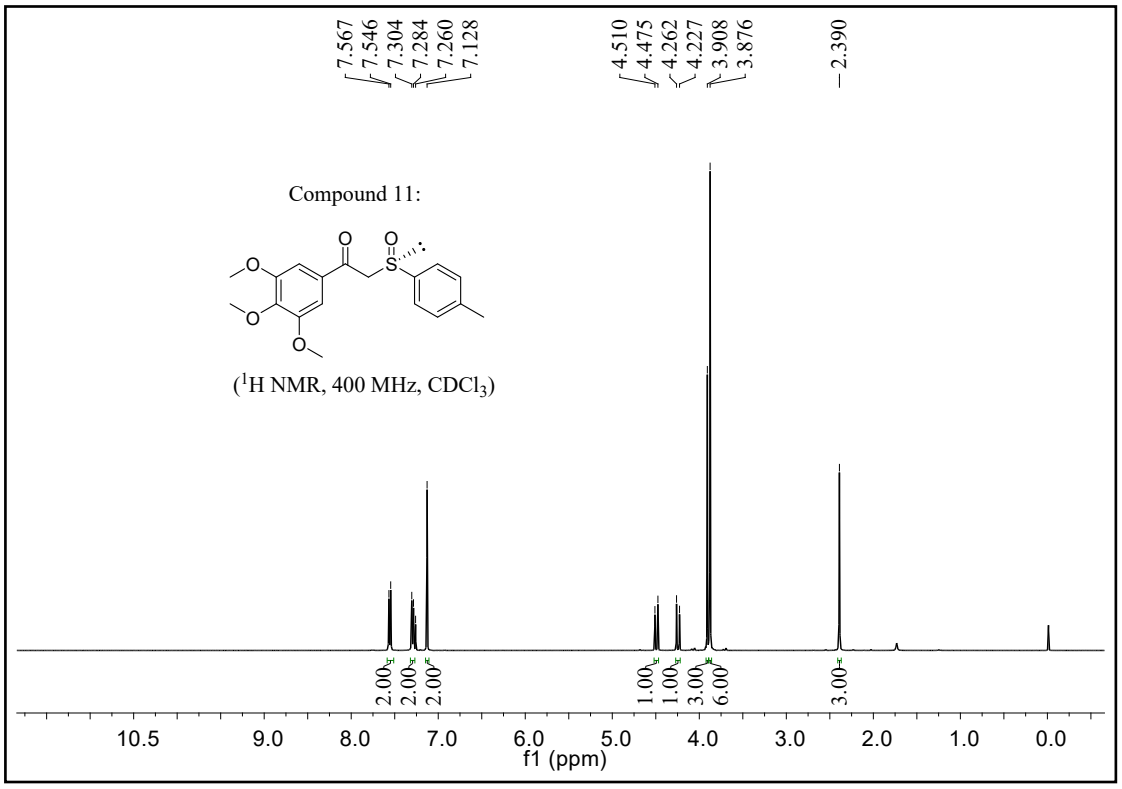

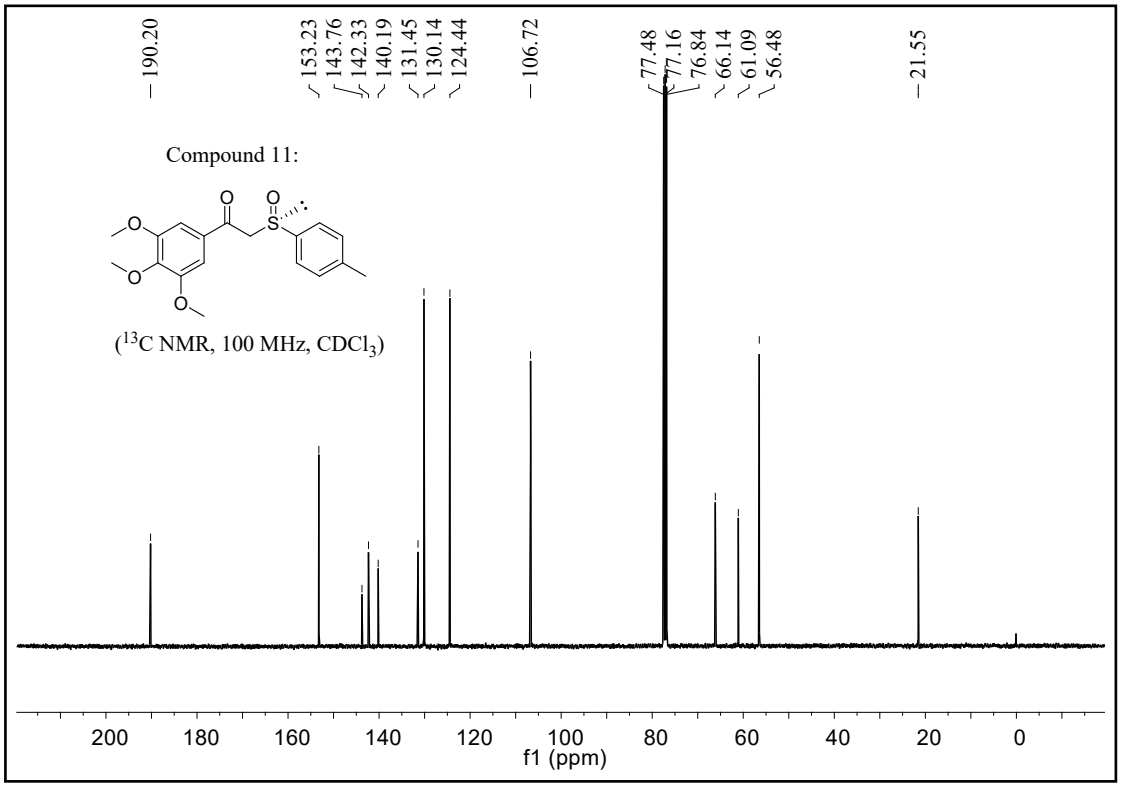

3-(4-Ethoxy-3-fluorophenyl)-4,5,6-trimethoxy-2-((*R*)-p-methylsulfoxide)-2,3-dihydro-1H-inden-1-one (**13**)

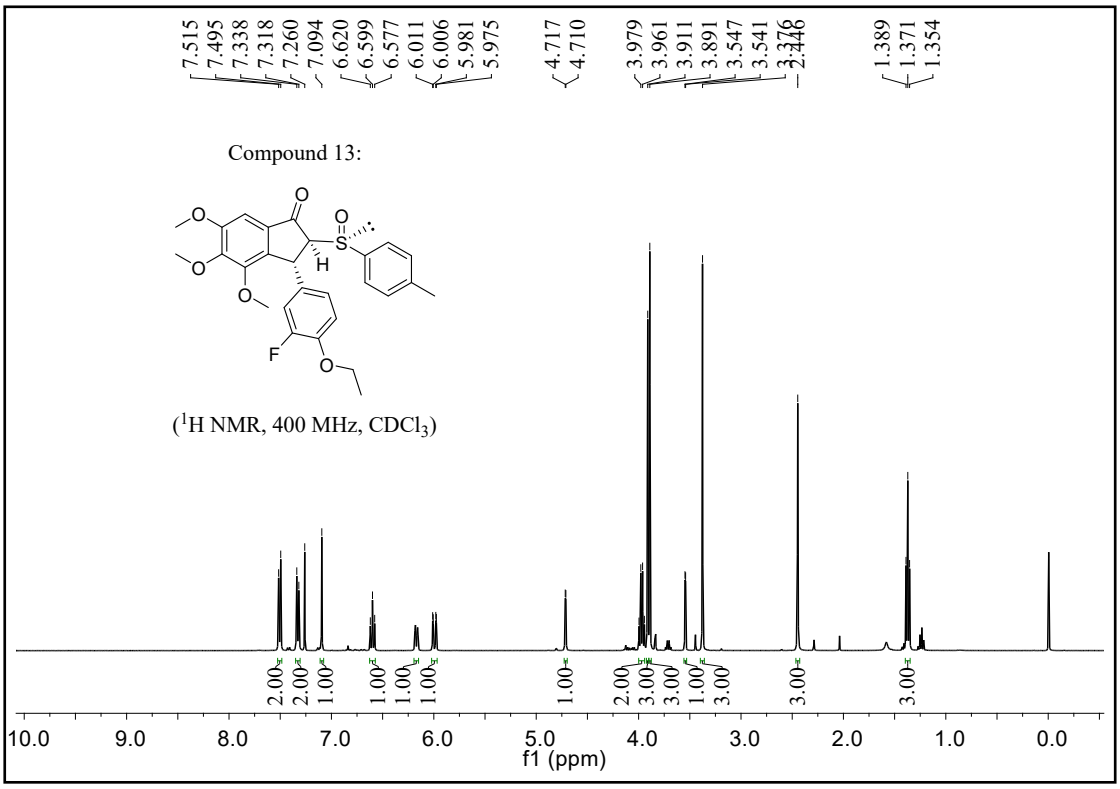

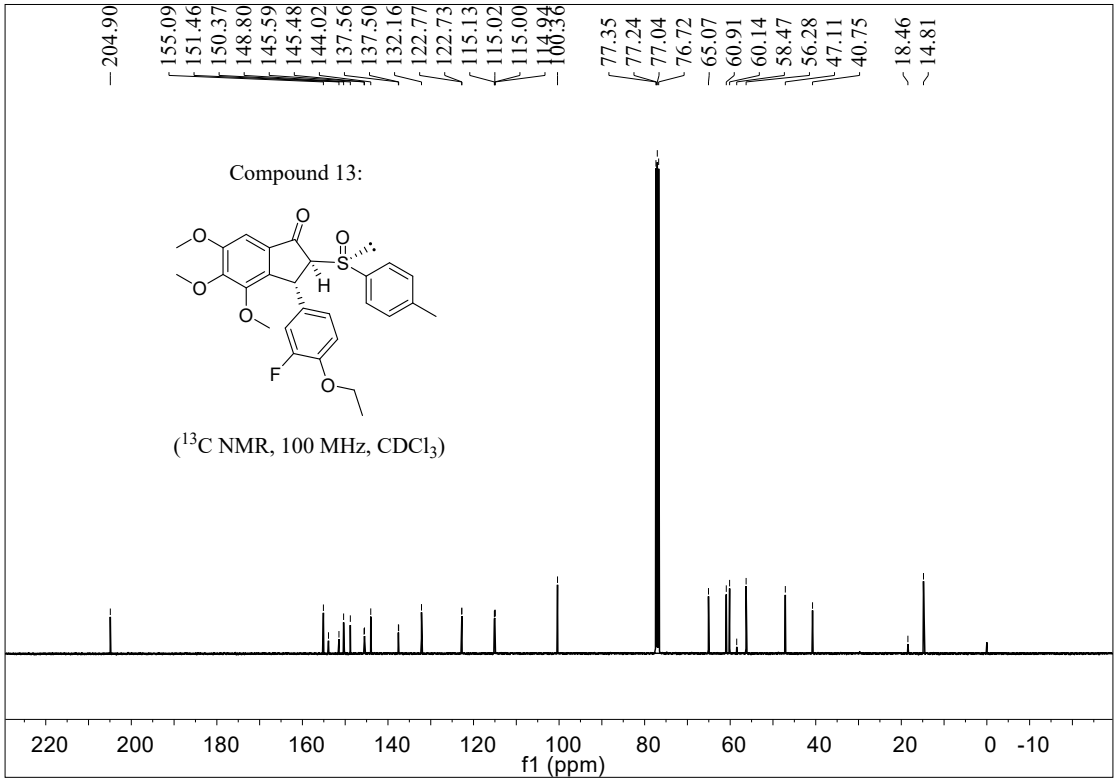

X-Ray Structures of **(*R*)-9k**.

ORTEP drawing of the X-ray crystallographic structure of compound **(*R*)-9k** (50% probability ellipsoids):

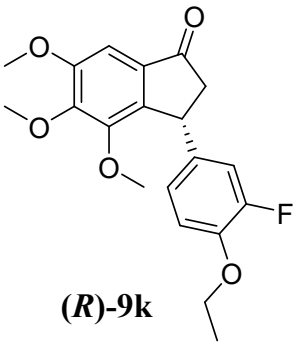

(*R*)-9k

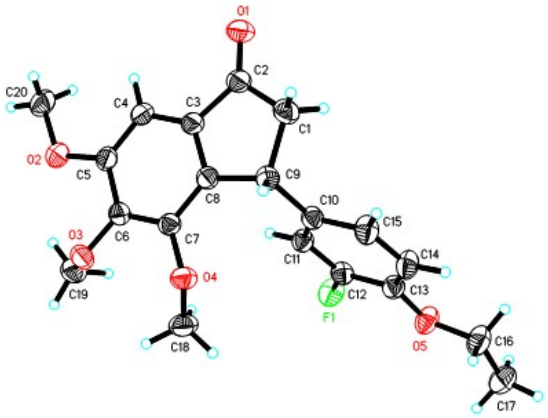

Identification code	**(*R*)-9k**
Empirical formula	$C_{20}H_{21}FO_5$
Formula weight	360.37
Temperature	293(2) K
Wavelength	1.54178 Å
Crystal system	Monoclinic
Space group	P 21
Unit cell dimensions	a = 14.3474(5) Å
	b = 4.42800(10) Å
	c = 14.8423(5) Å
Volume	886.60(5) $Å^3$
Z	2
Density (calculated)	1.350 Mg/m^3
Absorption coefficient	0.864 mm^{-1}
F(000)	380
Crystal size	0.190 x 0.100 x 0.070 mm^3
Theta range for data collection	8.214 to 66.387°.
Index ranges	-17<=h<=17, -5<=k<=4, -16<=l<=17
Reflections collected	10827
Independent reflections	2940 [R(int) = 0.0326]

Completeness to theta = 67.679°	92.7 %
Absorption correction	Semi-empirical from equivalents
Max. and min. transmission	0.7533 and 0.4831
Refinement method	Full-matrix least-squares on F^2
Data / restraints / parameters	2940/1/240
Goodness-of-fit on F^2	1.078
Final R indices [I>2sigma(I)]	R1 = 0.0320, wR2 = 0.0844
R indices (all data)	R1 = 0.0356, wR2 = 0.0872
Absolute structure parameter	0.08(5)
Extinction coefficient	0.037(8)
Largest diff. peak and hol 0.115 and -0.101 e.Å-3	0.115 and -0.101 e.$Å^{-3}$

CCDC 2180666. For detailed crystallographic data, please refer to the Cambridge Crystallographic Data Centre at http://ccdc.cam.ac.uk.